DATABASE ANALYSIS

e-ISSN 1643-3750
© Med Sci Monit, 2026; 32: e951911
DOI: 10.12659/MSM.951911

Received: 2025.10.27
Accepted: 2026.03.19
Available online: 2026.04.10
Published: 2026.XX.XX

ScRNA-seq Data Reveal Gene Upregulation and Downregulation in Oxygen-Induced Retinopathy

Authors' Contribution:
Study Design A
Data Collection B
Statistical Analysis C
Data Interpretation D
Manuscript Preparation E
Literature Search F
Funds Collection G

ABCE 1 Xinhe Wang
BCE 1 Lijie Wang
CDE 2 Yanhong Ju

1 Department of Ophthalmology, The Fourth People's Hospital of Shenyang, Shenyang, Liaoning, PR China
2 Outpatient Department, The Fourth People's Hospital of Shenyang, Shenyang, Liaoning, PR China

Corresponding Author: Xinhe Wang, e-mail: wxinhe2025@163.com
Financial support: None declared
Conflict of interest: None declared

Background: Retinopathy of prematurity is characterized by retinal vascular ischemia and hypoxia that lead to neovascularization, potentially causing retinal detachment and blindness. This study aimed to explore target genes involved in oxygen-induced retinopathy (OIR) through comprehensive single-cell RNA sequencing (scRNA-seq) data analysis.

Material/Methods: ScRNA-seq data of retinal tissues obtained from mice under normoxic and OIR conditions were retrieved from the Gene Expression Omnibus (GEO; accession number GSE150703). A suite of bioinformatics tools was used for data processing, cell clustering, cell type annotation, differential gene expression analysis, gene set enrichment analysis, and protein–protein interaction network prediction to identify key hub genes associated with OIR.

Results: Analysis of GSE150703 OIR mouse data identified 10 retinal cell types. These findings were supported by pathway enrichment analyses, including Gene Ontology and Kyoto Encyclopedia of Genes and Genomes, which indicated significant upregulation of Hnrnpu, Vamp2, Ybx1, Ywhab, and Csnk1a1, and downregulation of Xist and mt-Co1, among others. Interacting proteins from protein–protein interaction network studies identified major hub genes involving Srsf1, Srsf11, Sf3b1, and Hnrnpu, among others. Moreover, the research explored how mutations of Chchd10 and Sf3b1 influence the development of the disease and downregulation of mitochondrial-associated genes, such as lncRNA-Xist, Ndufs5, and mt-Co1, which may provide further insight into their roles in the pathogenesis of OIR.

Conclusions: The single-cell data analysis suggests that Hnrnpu, Vamp2, Ybx1, Ywhab, Csnk1a1, Pfkp, Rho, Srsf1, Srsf11, Mt1, Tpr, Hnrnpc, Chchd10, Sf3b1, Xist, Ndufs5, and mt-Co1 may be potential target genes in OIR in retinopathy of prematurity.

Keywords: Retina • Retinopathy of Prematurity • Enrichment Analysis • PPI • Hub Genes • Oxygen-Induced Retinopathy

Full-text PDF: https://www.medscimonit.com/abstract/index/idArt/951911

Indexed in: [Current Contents/Clinical Medicine] [SCI Expanded] [ISI Alerting System] [ISI Journals Master List] [Index Medicus/MEDLINE] [EMBASE/Excerpta Medica] [Chemical Abstracts/CAS]

Introduction

Retinopathy of prematurity (ROP) is a vascular disease in premature infants characterized by pathological retinal neovessels, retinal vascular dilation, and hemorrhage, which could lead to retinal detachment and blindness [1]. Its uniqueness lies in the concurrent physiological and pathological angiogenesis in the developing retina, providing a unique model for studying angiogenesis regulation [2-4]. Pathological angiogenesis is a core feature of ROP, and understanding its molecular mechanisms is vital for developing treatment strategies for various diseases [2-4]. The most widely used oxygen-induced retinopathy (OIR) model has enabled the study of the pathophysiological processes occurring in ROP, uncovering both the mechanisms behind ROP and potential therapeutic interventions [5].

Current ROP screening methods require substantial resources in terms of equipment and ophthalmologist expertise, while biomarkers with high sensitivity and specificity offer a more convenient approach for early detection [6]. The interaction of different cell types and the regulation of various genes contribute to the development of pathological angiogenesis of ROP [4,6]. Therefore, exploring the gene regulations in ROP can aid in more precisely targeted therapies.

Single-cell RNA sequencing (scRNA-seq) has revolutionized the study of gene expression at a cellular resolution [7]. The advantage of scRNA-seq lies in its ability to discover rare cell types and track cell differentiation pathways, thereby enhancing the understanding of complex biological systems and disease mechanisms [7,8]. Some studies have used scRNA-seq to characterize the signal pathways or gene regulations associated with retinopathy and its relative therapies. This includes investigating how these pathways affect retinal neovascularization and promote retinal neurodegeneration [9,10].

However, research on gene regulation in OIR using scRNA-seq remains limited. This study investigated gene regulation in OIR rat models using data obtained from the Gene Expression Omnibus (GEO) platform. The key genes identified may serve as valuable risk biomarkers to enhance ROP screening.

Material and Methods

Data Download

The data set GSE150703 and annotation file GPL19057 were downloaded from the GEO data platform. GSE150703 contains 12 samples of retinal tissues obtained from mice under normoxic (NORM) conditions and OIR conditions on postnatal days 14 and 17. In this bioinformatics analysis, the data of the animals retrieved from the database were divided into 4 groups: P14-NORM (n=2), the NORM control group on postnatal day 14; P14-OIR (n=5), the OIR group on postnatal day 14; P17-NORM (n=2), the NORM control group on postnatal day 17; and P17-OIR (n=3), the OIR group on postnatal day 17.

This research is a bioinformatics analysis and ethical approval certification is not required. The relevant data for the research was obtained from the database and analyzed.

Quality Control

The R package DropletUtils [11] was used to determine the expression levels in each cell, and barcodes were filtered. The cells were further filtered according to the number of unique molecular identifiers in each cell. Then, the scater [12] package was used to quantify the expression of genes in cells, and the cells were filtered based on the proportion of mitochondrial gene reads (<10%), as shown in **Figure 1A-1C**. We retained those cells whose proportion of mitochondrial gene-encoded unique molecular identifiers (percent.mt) was less than 20% and whose detected number of genes (nFeature_RNA) was greater than 200 and less than 6000, as well as those with a total unique molecular identifier count (nCount_RNA) greater than 500 for further analysis.

Data Preprocessing

The NormalizeData function in the Seurat [13] package was used to normalize the expression matrix of each sample after filtering.

Principal Component Analysis

The 2000 genes with the greatest differential expression between cells were identified by using the FindVariableFeatures function in the Seurat package. Then, the ScaleData function in the Seurat package was used to linearly scale the expression data. Finally, the RunPCA function in the Seurat package was used for linear dimensionality reduction analysis, as shown in **Figure 1D-1G**.

Cell clustering and Annotation

We selected the principal component with the highest standard deviation and used the FindNeighbors and FindClusters functions in the Seurat package for cell cluster analysis. Then, the RunUMAP function in the Seurat package was used for nonlinear dimensionality reduction analysis, as shown in **Figure 1H and 1I**.

Identification of Marker genes

The FindMarkers function in the Seurat package was used to identify the differentially expressed genes (DEGs) between

Indexed in: [Current Contents/Clinical Medicine] [SCI Expanded] [ISI Alerting System] [ISI Journals Master List] [Index Medicus/MEDLINE] [EMBASE/Excerpta Medica] [Chemical Abstracts/CAS]

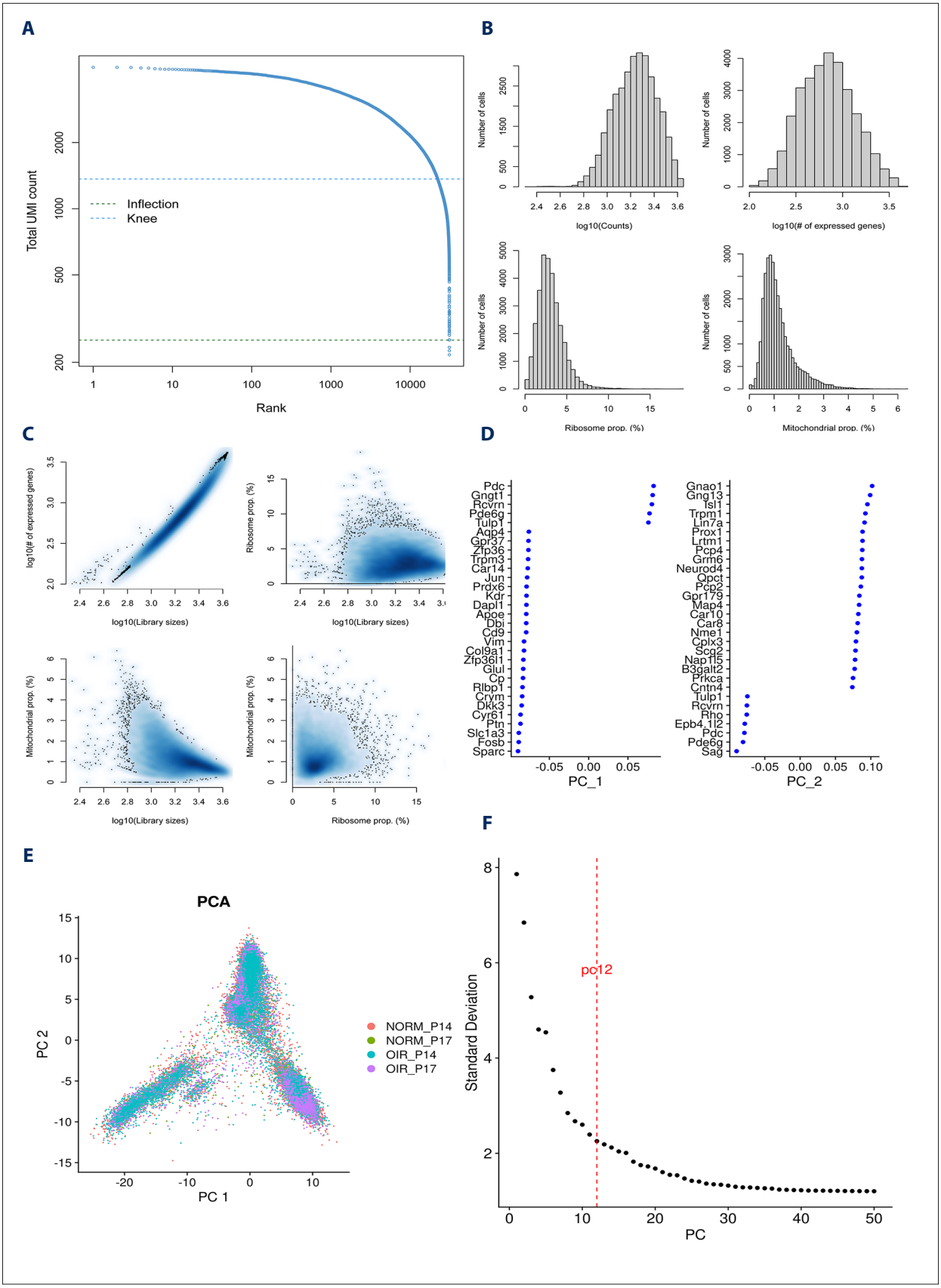

Indexed in: [Current Contents/Clinical Medicine] [SCI Expanded] [ISI Alerting System] [ISI Journals Master List] [Index Medicus/MEDLINE] [EMBASE/Excerpta Medica] [Chemical Abstracts/CAS]

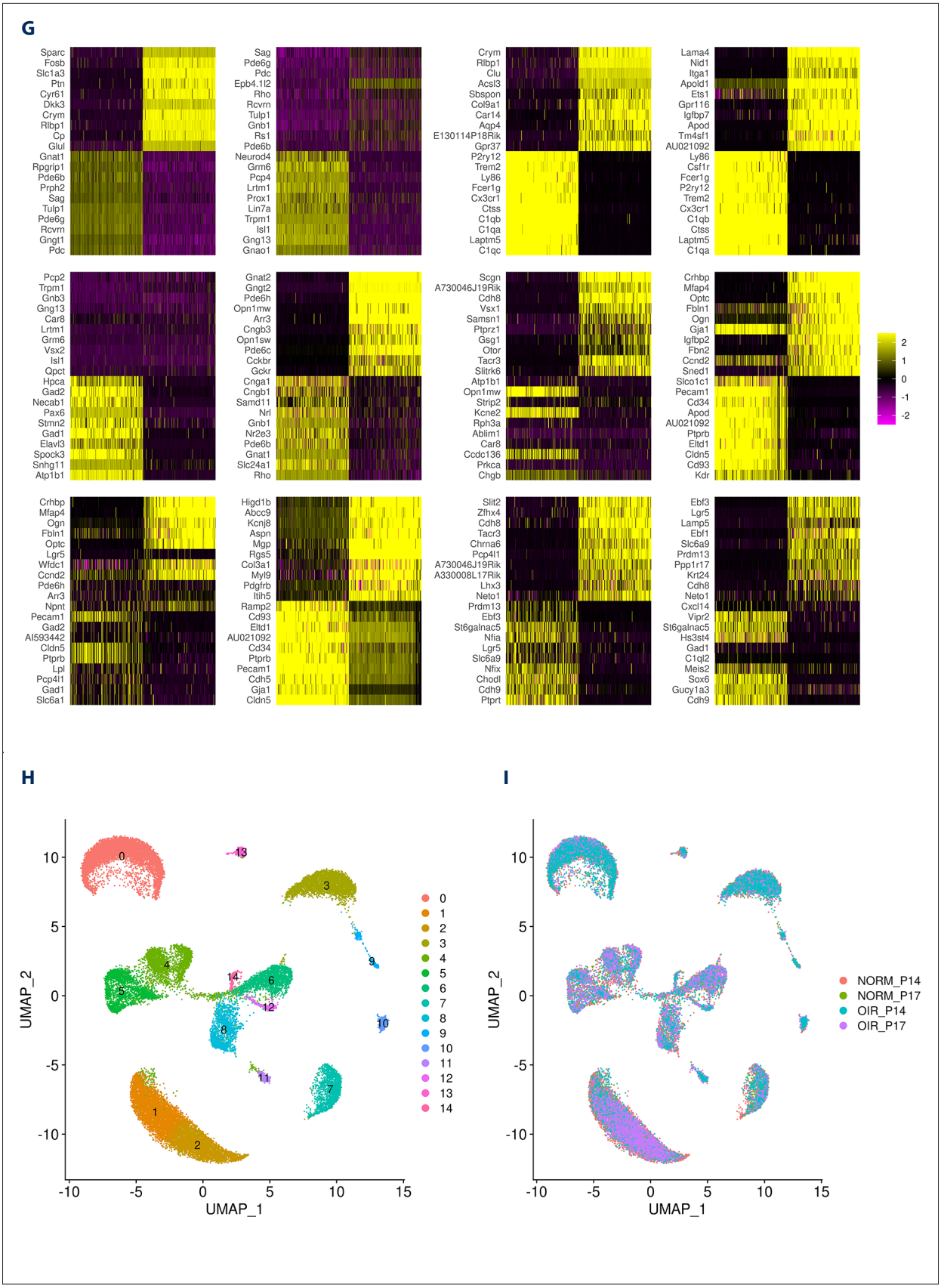

Indexed in: [Current Contents/Clinical Medicine] [SCI Expanded] [ISI Alerting System] [ISI Journals Master List] [Index Medicus/MEDLINE] [EMBASE/Excerpta Medica] [Chemical Abstracts/CAS]

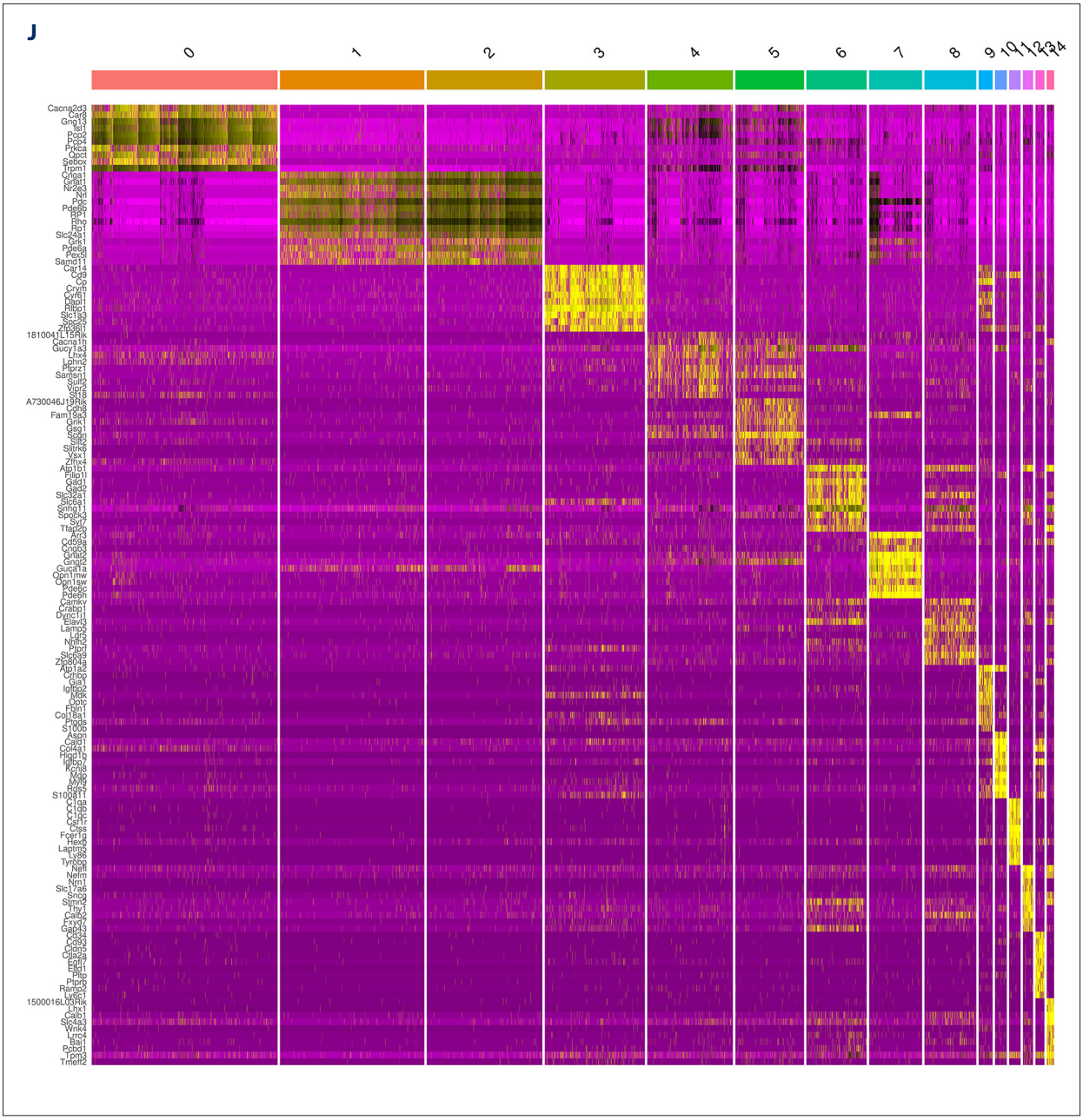

Indexed in: [Current Contents/Clinical Medicine] [SCI Expanded] [ISI Alerting System] [ISI Journals Master List] [Index Medicus/MEDLINE] [EMBASE/Excerpta Medica] [Chemical Abstracts/CAS]

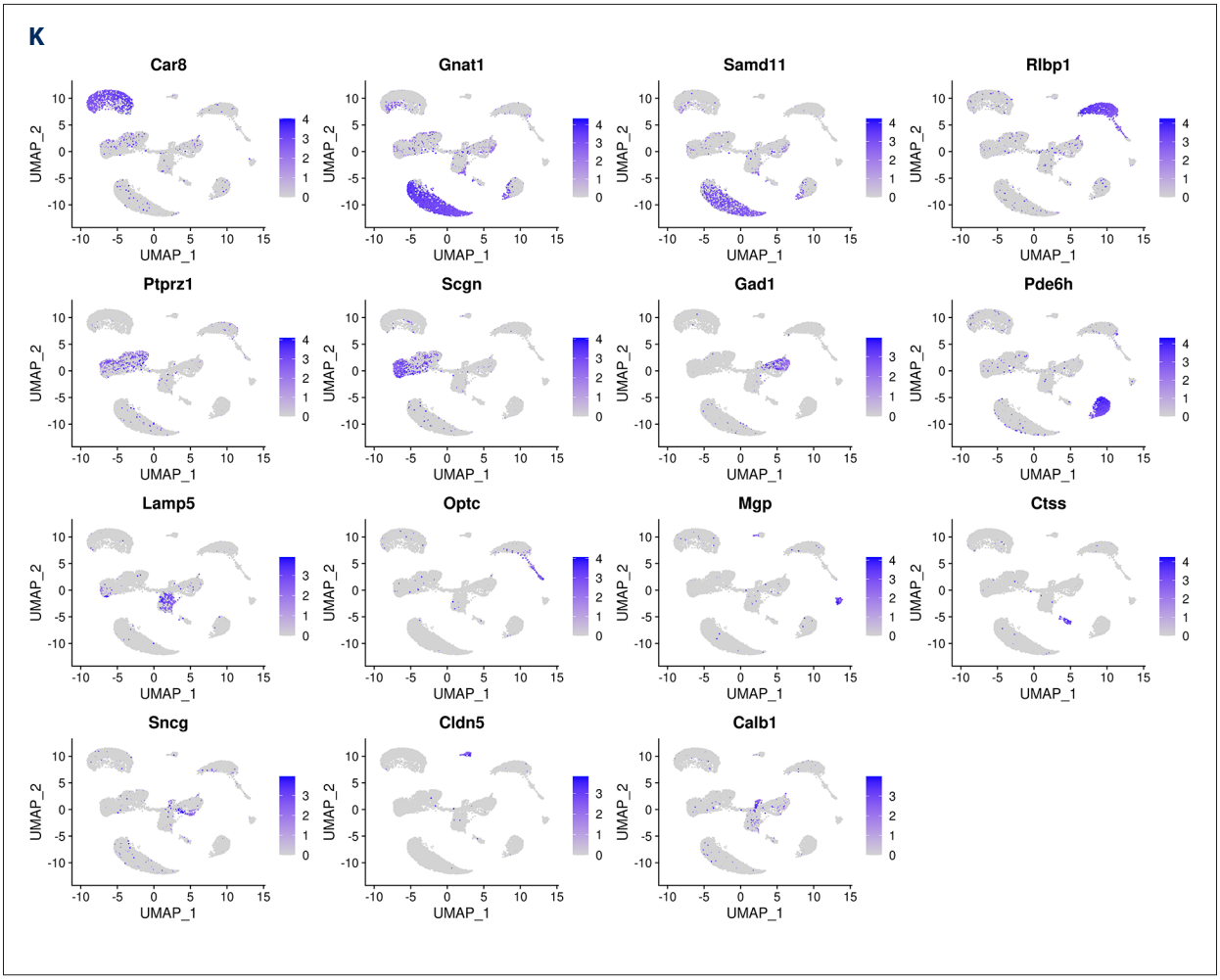

Figure 1. (**A**) Barcode rank plot showing gene expression counts after sequencing. (**B**) Statistical chart of gene expression. (**C**) Proportion of various genes. (**D**) Top 2 principal component (PC) gene contribution values. (**E**) Principal component analysis (PCA) plot. (**F**) PC plot of the top 12 PCs. (**G**) Heatmap of the top 12 PCs. (**H**) Uniform manifold approximation and projection (UMAP) cell cluster diagram. (**I**) UMAP cell grouping diagram. (**J**) Heatmap of the top 10 marker genes in each cluster; each row represents 1 gene, and each column represents 1 cell cluster. (**K**) Expression map of the top marker gene in each cluster.

the cells in each cluster and all other cells (log2 fold change [FC] ≥2; *P* value ≤0.05) to identify marker genes (the top 500 ranked by logFC). The cells were labelled according to the existing marker [14] genes, and a cluster diagram was generated, as shown in **Figure 1J and 1K**. We used the FindMarkers function in the Seurat package for differential expression analysis, and the minimum expression ratio in the cell population was set at 0.25.

Gene Enrichment Analyses

Based on the GO [15] database and Kyoto Encyclopedia of Genes and Genomes (KEGG) pathway database [16], functional enrichment analyses were performed with the candidate genes. GO enrichment analysis was performed to discover the biological processes enriched with these DEGs and demonstrated the important functions of the differential gene expression among the groups. GO enrichment analysis consists of 3 categories: biological processes, cellular components, and molecular functions.

Protein–protein interaction network prediction

The protein–protein interactions (PPIs) of the proteins encoded by the candidate genes were analyzed using the STRING [17] online tool. In this study, a required confidence level (combined score) of >0.7 was selected as the PPI threshold. By connectivity degree analysis of the network statistics, the hub proteins, important nodes involved in the protein interactions in the PPI network, were identified.

Indexed in: [Current Contents/Clinical Medicine] [SCI Expanded] [ISI Alerting System] [ISI Journals Master List] [Index Medicus/MEDLINE] [EMBASE/Excerpta Medica] [Chemical Abstracts/CAS]

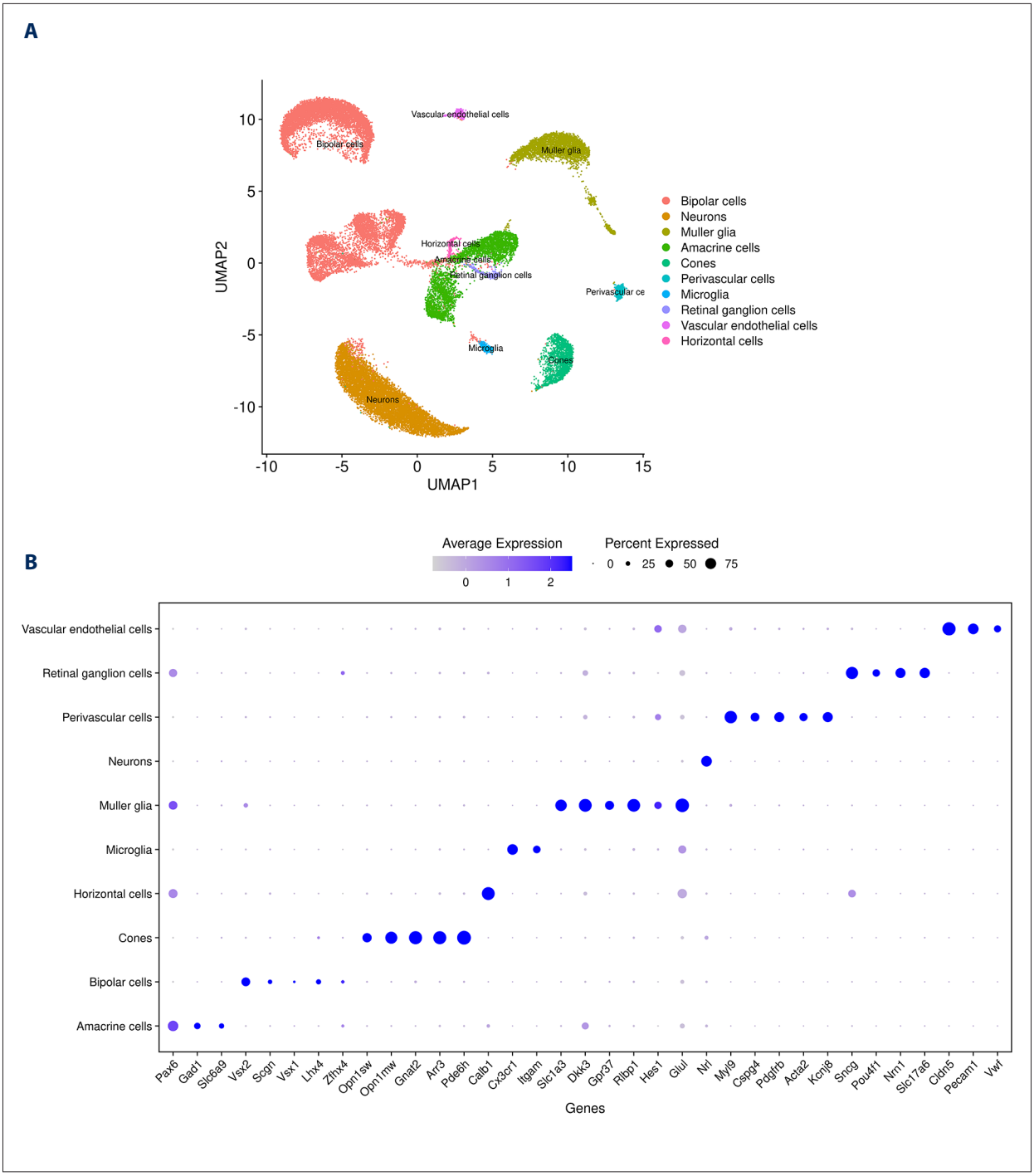

Indexed in: [Current Contents/Clinical Medicine] [SCI Expanded] [ISI Alerting System] [ISI Journals Master List] [Index Medicus/MEDLINE] [EMBASE/Excerpta Medica] [Chemical Abstracts/CAS]

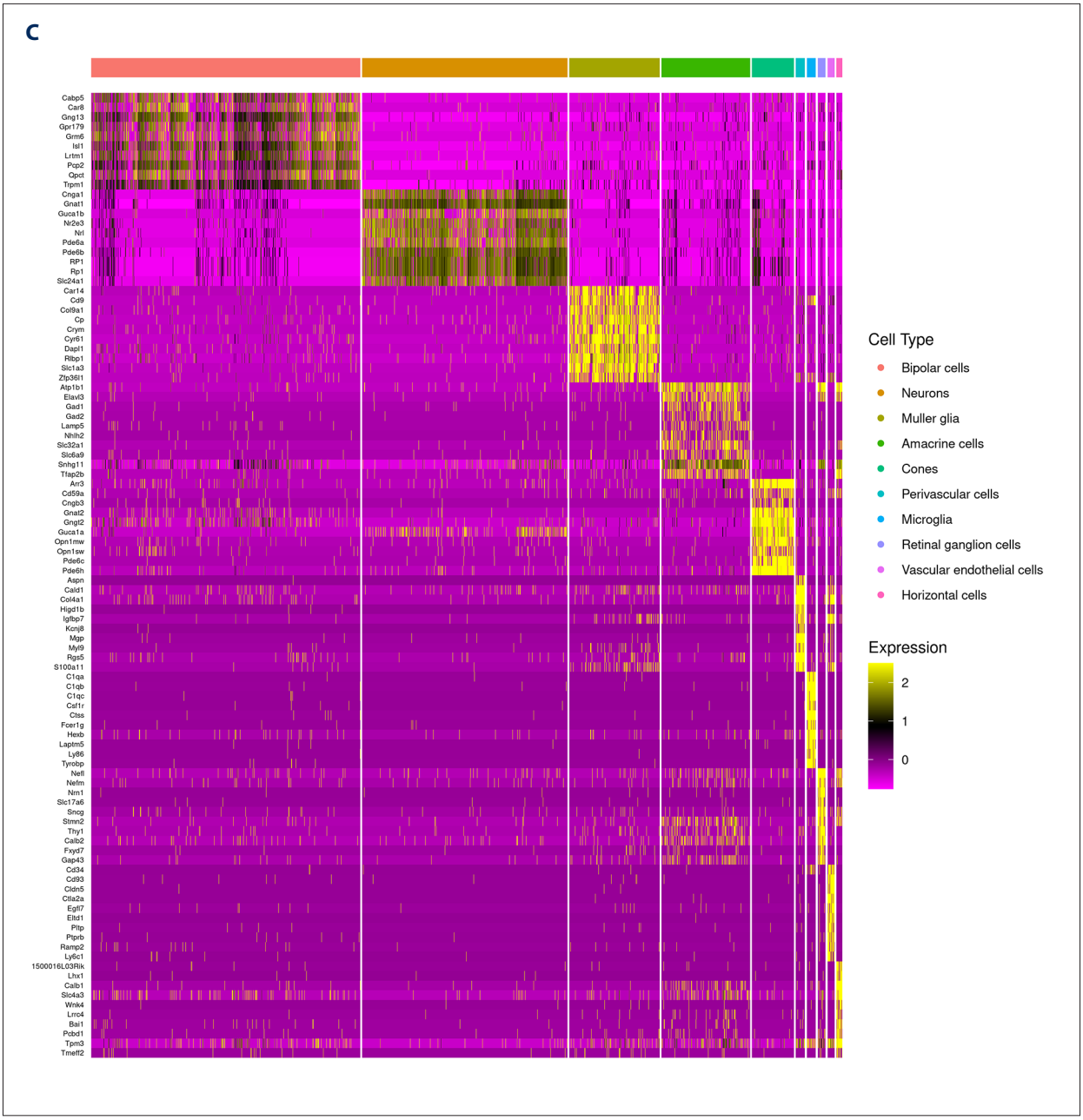

Indexed in: [Current Contents/Clinical Medicine] [SCI Expanded] [ISI Alerting System] [ISI Journals Master List] [Index Medicus/MEDLINE] [EMBASE/Excerpta Medica] [Chemical Abstracts/CAS]

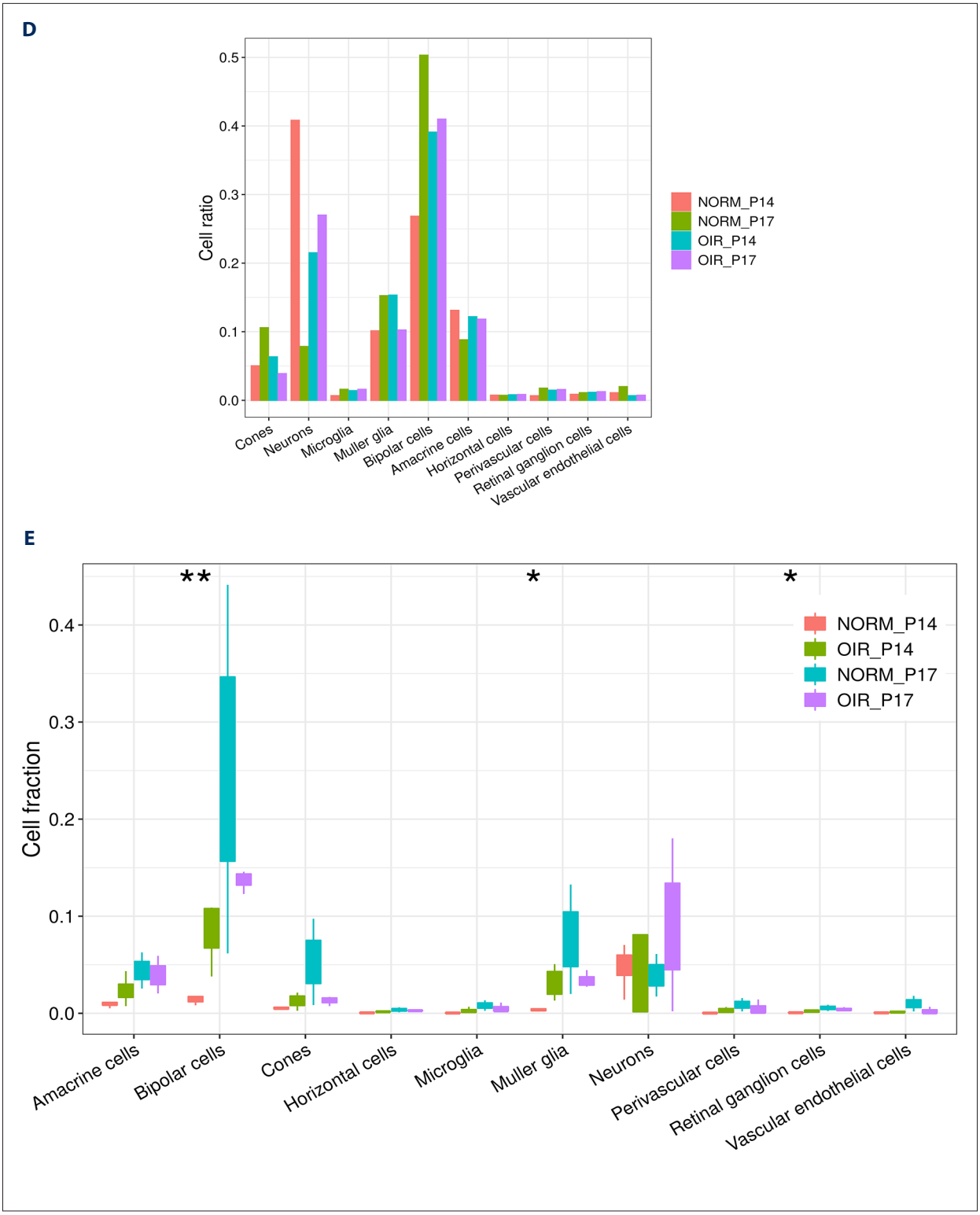

Figure 2. (**A**) Cell types of each cluster. (**B**) Expression of marker genes used to identify various cell types. (**C**) Heatmap of the top 10 newly identified marker genes in different cell types. (**D**) Proportion of each cell type in grouped samples. (**E**) Results of cell proportion analysis. On the left side of the vertical line, OIR_P14 vs NORM_P14; on the right side, OIR_P17 vs NORM_P17. * $P<0.001$, $0.01\leq P<0.05$. OIR – oxygen-induced retinopathy; NORM – normoxic; P14 – postnatal day 14; P17 – postnatal day 17.

Indexed in: [Current Contents/Clinical Medicine] [SCI Expanded] [ISI Alerting System] [ISI Journals Master List] [Index Medicus/MEDLINE] [EMBASE/Excerpta Medica] [Chemical Abstracts/CAS]

Table 1. Differential gene expression analysis results.

Data information		Difference threshold		Number of differential genes		Cell number	
Data source	Platform	FC	q value	Upregulated	Downregulated	OIR-P17	NORM-P17
GSE150703	NextSeq	2	0.05	355	5	374	50

FC – fold change; OIR – oxygen-induced retinopathy; NORM – normoxic; P17 – postnatal day 17.

Table 2. Differential expression of genes.

	Gene name
Downregulated genes	mt-Co1, Xist, Tma7, Sebox, Ndufs5
Upregulated genes	D4Wsu53e, Rho, Ywhab, E130218I03Rik, Hnrnpu, Vamp2, Csnk1a1, Pfkp, Ybx1, Bsg, Ptms, Atxn7l3b, Luc7l3, Pafah1b1, Chchd10, Pcbp2, Srrm3, Bin1, Zmiz1, Pitpnm1, Purb, Plk5, Srrm2, Klc1, Cox5a, Eid1, Sfpq, Rtn3, Slc12a5, Nisch, Pura, Acaa1a, Stx3, Ddx17, Tspan3, Kmt2c, Uqcrfs1, Mrfap1, Thsd7a, Atxn2l, Pdcd4, Gnat1, Amy1, Aldoc, Cpe, Phip, Kif5c, Zmynd11, Abhd8, Rpgrip1, Zcrb1, Nucks1, Srsf2, Clta, Srsf11, Hnrnpd, Tpr, Smarca2, Arglu1, Chd4, Safb, Rtf1, Baz2b, Kif1b, Sqstm1, Rbm39, Mycbp2, Hook1, Smarcc2, Atp1a3, Dcaf7, Gnb1, Ttc14, Itm2b, Ctnnb1, Hmgn1, Hif1a, Serbp1, Fam193b, Eif5, Ubxn4, Cyc1, Atp1b2, Pcm1, BC005537, Kif21a, Akap9, Fth1, Slc25a3, Rps2, Mlf2, Slc6a6, Dnajc5, Fkbp4, Ccdc88a, Srsf1, Golga4, Gls, Eif4g3, Fam171b, Rab14, Ap3d1, Bclaf1, Prrc2c, Madd, Ythdc1, Sv2a, Khdrbs3, Tra2a, Ubtf, Akap11, Baz1b, Crmp1, Nipbl, Desi1, Pacsin1, Ttc3, Dnmt3a, Rbbp6, Ash1l, Stxbp1, Unc119, Hnrnph3, Ncor1, Mff, Hnrnpl, Gsk3b, Mpp4, Nr1d2, Slc1a2, Hsp90b1, Agap1, Atrx, Sag, Sptbn1, Rnf187, Pabpc1, Psip1, Pnn, Brd2, Senp6, Dynll2, Gnb2l1, Cd47, Prrc2b, Gtf2i, Ank2, Ctbp2, Strbp, Kmt2e, Ccnl2, Gm16586, Zc3h7a, Nktr, Ccnl1, Akap8l, Rab2a, Snap91, Npepps, Tnrc6a, Rrp1, Mapre3, Cadm1, Ddx6, Ankrd11, Gucy1a3, Ik, Zfp91, Fscn1, Srrm1, Luc7l2, Ubn2, Nlk, Ccar1, Tia1, Vegfa, Prpf38b, Fnbp4, Fam168a, Canx, Nrxn3, Stub1, Vezf1, Tmem66, Ldha, Zcchc11, Fus, Zfp292, Ktn1, Msl1, App, Pdia3, Msi2, Cep290, Nap1l1, Phyhipl, Mtdh, Zdhhc17, Hnrnpc, Zfp106, Sbno1, Tjp2, Rpl13, Atp2b1, Sf3b1, Zranb1, Kmt2a, Zmynd8, Apc, Macf1, Ttyh1, Top2b, Arpc2, Fubp1, Fkbp1a, 2700089E24Rik, Clk4, Wdr26, Hsp90ab1, Necap1, Smug1, Thoc2, Jhdm1d, Fip1l1, Gnas, Spop, Ptprd, Eif4g1, Rora, Nol7, Setd5, Dgkd, Ppig, Rsrc2, Sltm, Ddx1, Zfr, Ppp1r12c, Gngt1, Eif3a, Rufy3, Camsap2, Ctr9, Sf3b2, Ddx46, Sf1, Zc3h13, Pfkl, Ndnf, Oxct1, Dot1l, Rb1cc1, Riok3, Dhx15, Htatsf1, Matr3, Acin1, Lman1, Cadm3, Anp32e, Smarca4, G3bp2, Samd14, Hnrnph1, H2afv, Rdx, Gnl3l, Lbh, Tnrc6b, Mt1, Pgm2l1, Bod1l, Tbl1x, Rps21, Map2k7, Fam162a, Runx1t1, Celf1, Top1, Tax1bp1, Jmjd6, Dhx36, Map7d2, Kifap3, Smap1, Ndufab1, Nsd1, Soga3, Dnaja2, Myo5a, Eif3c, Ggnbp2, Ahi1, Eprs, Cul5, Hnrnpm, Osbpl6, Chd9, Ddx42, Bhlhe23, Zc3h15, Fkbp3, Hnrnpa3, Sfrs18, Thoc7, Ankrd12, Eif5a, Smc3, Plcb4, Rsf1, Bnip3, Rev3l, Dnm1l, Tfrc, Sgip1, Cdk11b, Arhgef9, Scd2, Zfp326, Mia3, Hlf, Calr, Pfn1, Slk, Ncl, Dync1i2, Arid4b, Taf1, Cbx5, Rabl6, Drap1, Lpgat1, Auts2, Tubb2a, Anp32a, Gria2, Nfe2l1, Ckap5, Glrx2, Tial1, Syne1, Cxx1b, Eif5b, Mt2, Ivns1abp, Prox1, Tlk2, Gramd1b, R3hdm1, Arid4a, Lhx4, Cfdp1, Ccdc136, Vstm2b

Results

Identification of Cell Types

The cell type in each cluster was determined based on the marker gene for each cell and the marker gene for each cell cluster. We identified 10 kinds of cells: bipolar cells, neurons, Muller glia, amacrine cells, cones, perivascular cells, microglia, retinal ganglion cells, vascular endothelial cells, and horizontal cells, as shown in **Figure 2A and 2B**. Then, the marker genes of all these cell types were reanalyzed to identify new marker genes, as shown in **Figure 2C**.

Analysis of Cell Proportions

The proportions of the types of cells in each sample with respect to the corresponding total number of cells were determined, as shown in **Figure 2D**. Then, the *t* test was used to determine the significance of the differences in the corresponding comparisons, as shown in **Figure 2E**. **Figure 2D and 2E** showed that there were significant differences among 3 kinds of cells: bipolar cells ($P<0.001$), Muller glia ($P=0.027$), and retinal ganglion cells ($P=0.043$). According to the results of the above analysis, we selected the most significantly different cells, bipolar cells, as the core cells for subsequent analyses. Bipolar cells act as relay stations for retinal signal transmission and sensitive nodes for energy metabolism for OIR. Bipolar cells

Indexed in: [Current Contents/Clinical Medicine] [SCI Expanded] [ISI Alerting System] [ISI Journals Master List] [Index Medicus/MEDLINE] [EMBASE/Excerpta Medica] [Chemical Abstracts/CAS]

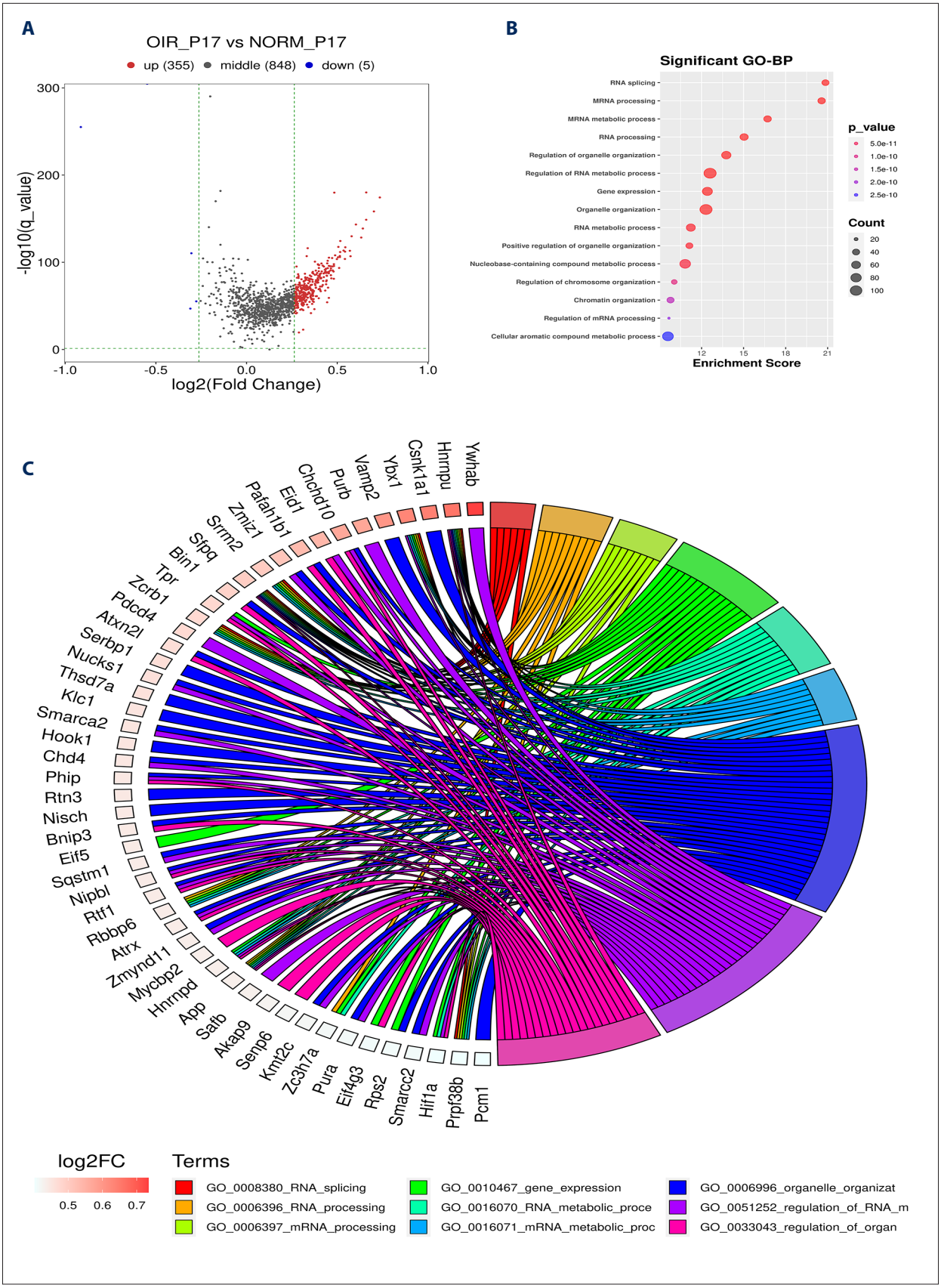

Indexed in: [Current Contents/Clinical Medicine] [SCI Expanded] [ISI Alerting System] [ISI Journals Master List] [Index Medicus/MEDLINE] [EMBASE/Excerpta Medica] [Chemical Abstracts/CAS]

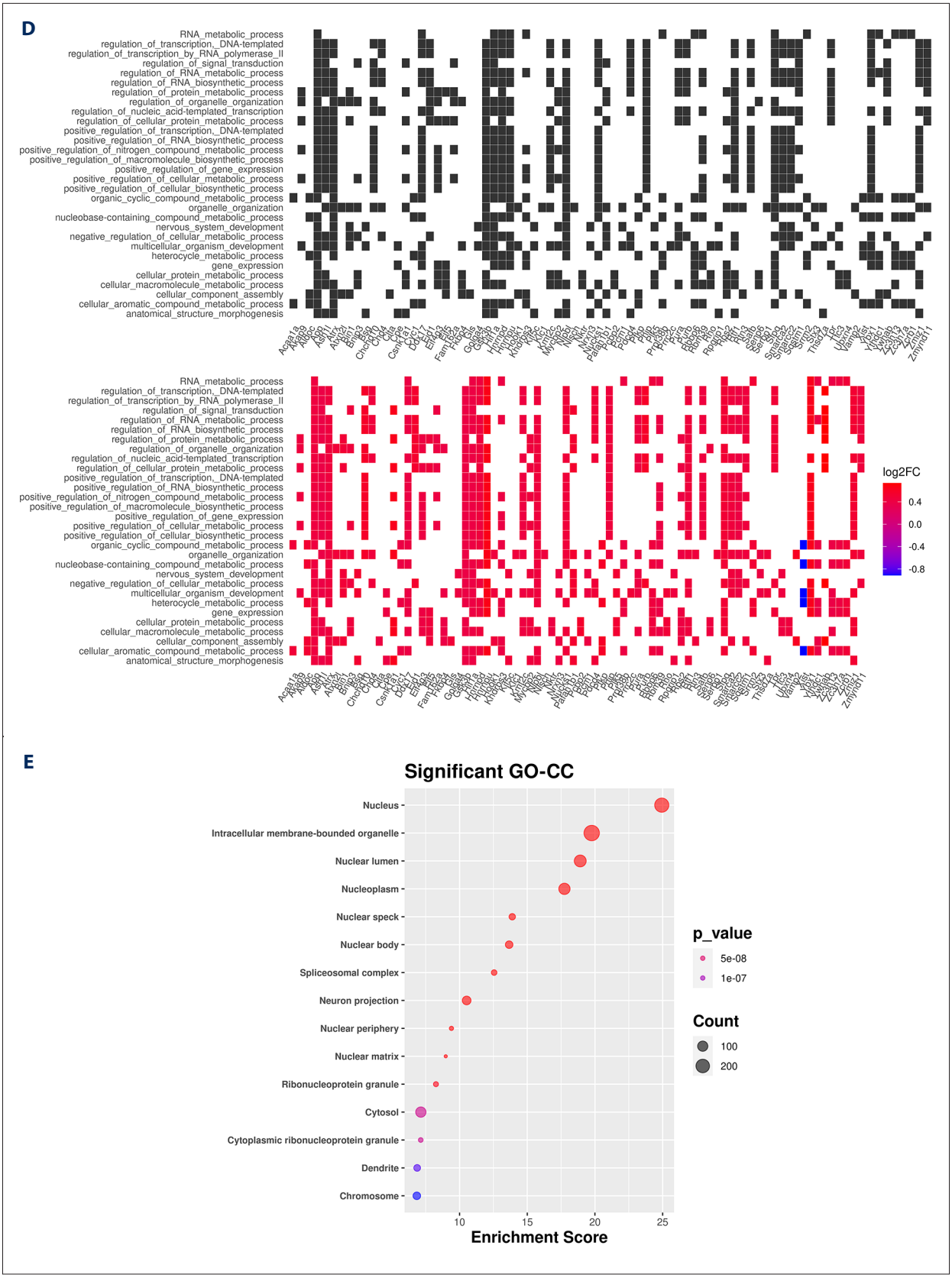

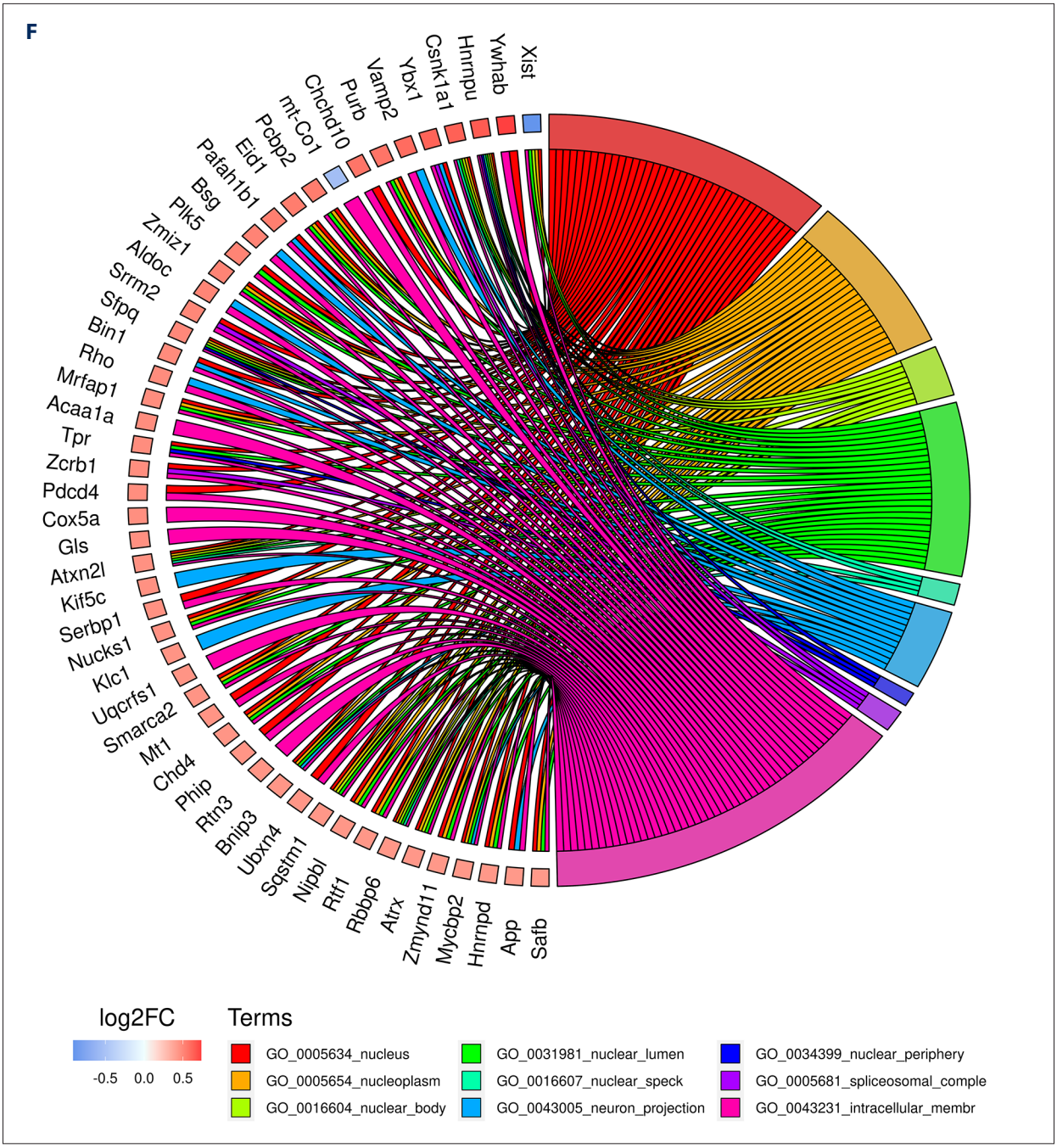

Indexed in: [Current Contents/Clinical Medicine] [SCI Expanded] [ISI Alerting System] [ISI Journals Master List] [Index Medicus/MEDLINE] [EMBASE/Excerpta Medica] [Chemical Abstracts/CAS]

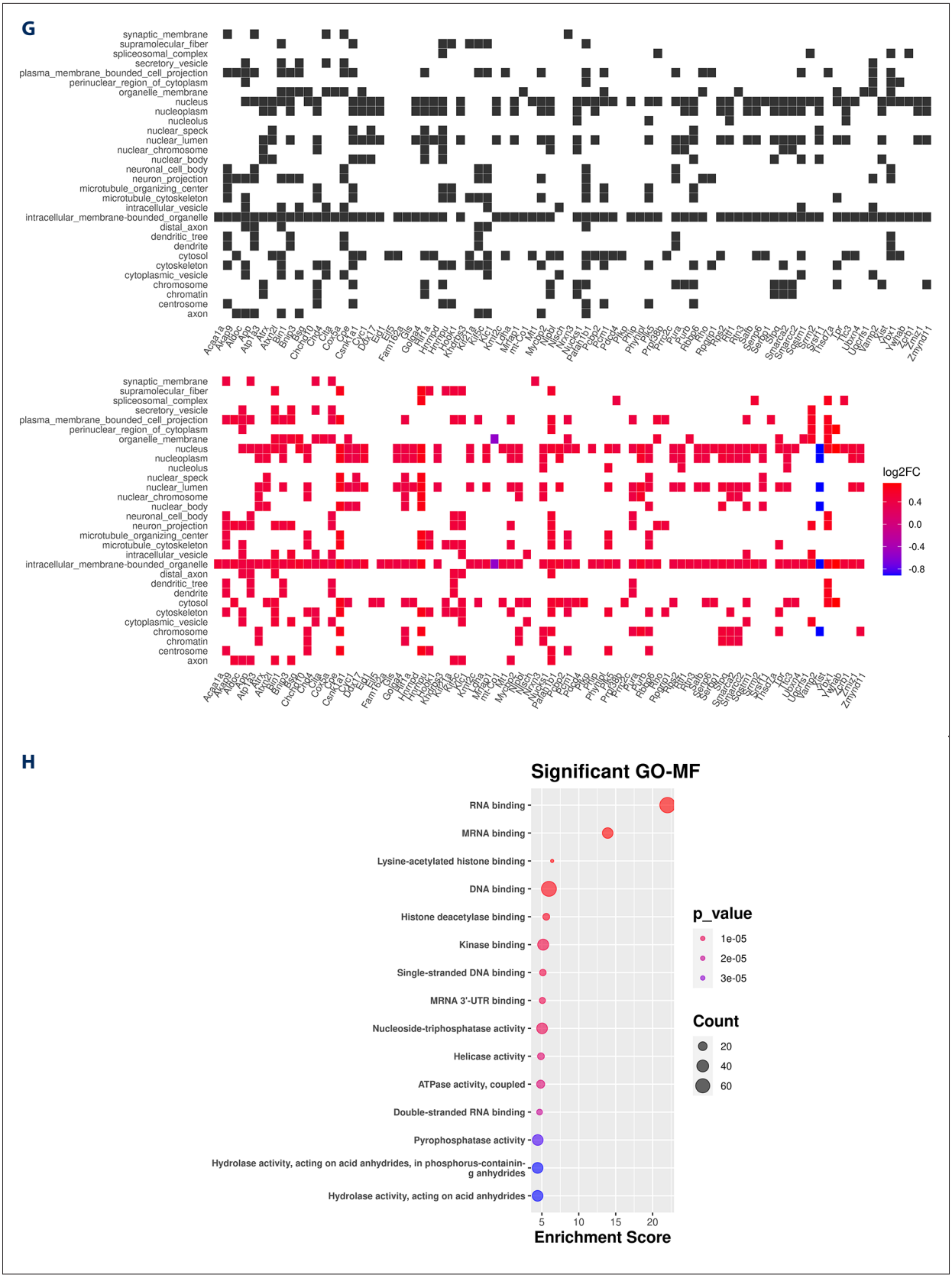

Indexed in: [Current Contents/Clinical Medicine] [SCI Expanded] [ISI Alerting System] [ISI Journals Master List] [Index Medicus/MEDLINE] [EMBASE/Excerpta Medica] [Chemical Abstracts/CAS]

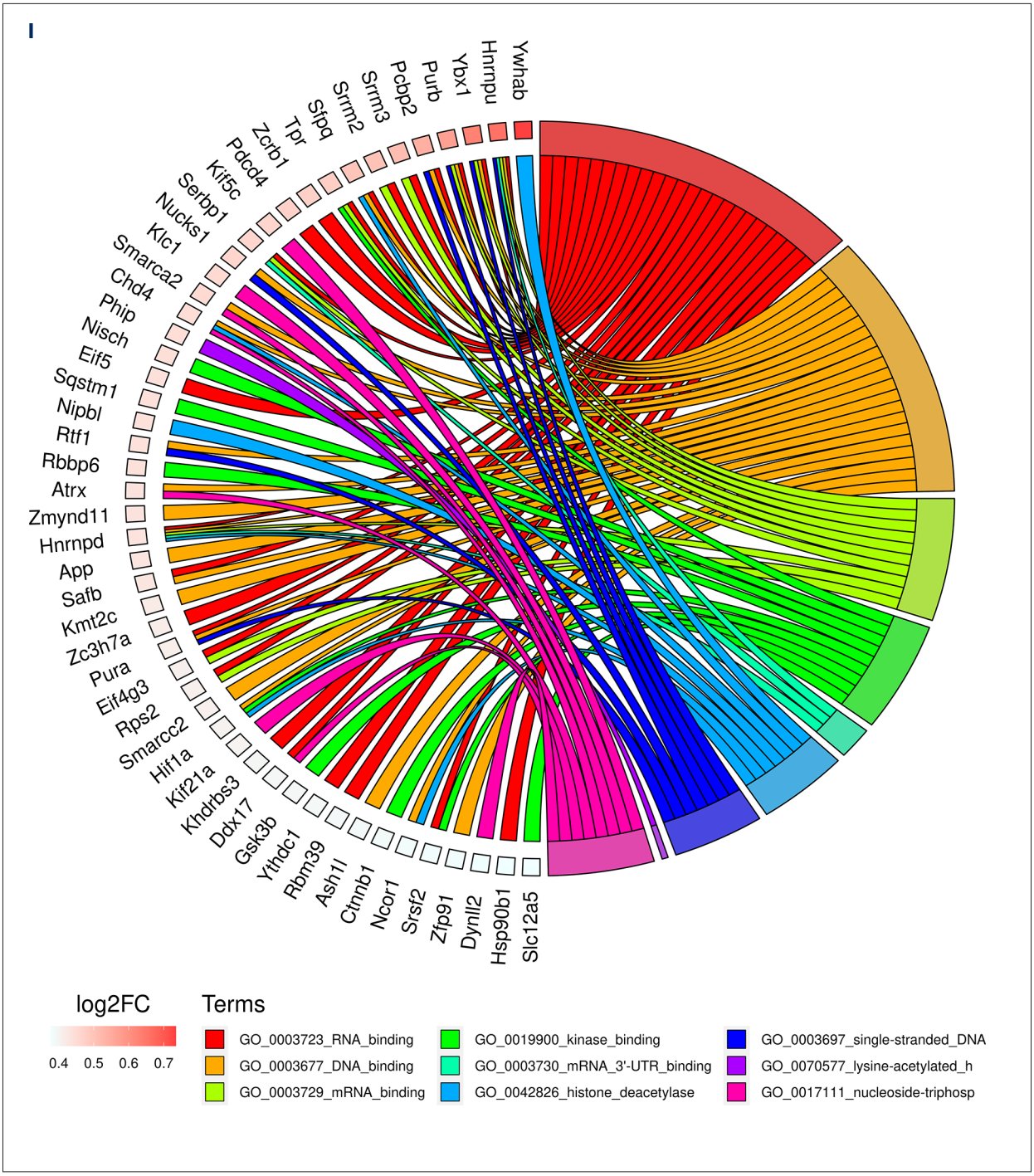

Indexed in: [Current Contents/Clinical Medicine] [SCI Expanded] [ISI Alerting System] [ISI Journals Master List] [Index Medicus/MEDLINE] [EMBASE/Excerpta Medica] [Chemical Abstracts/CAS]

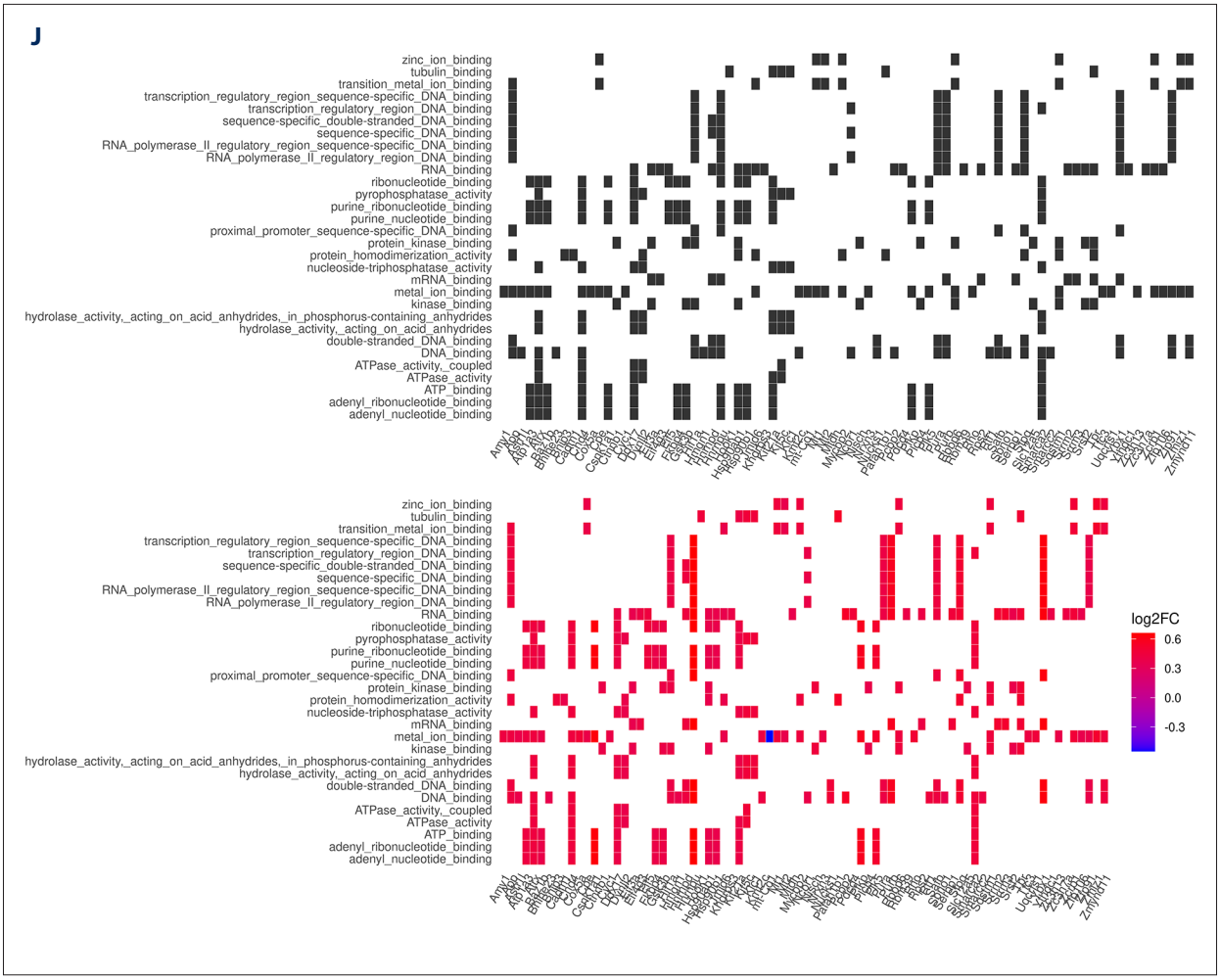

Figure 3. (**A**) Volcano plot of differentially expressed genes (DEGs) in bipolar cells (q<0.05 and fold change [FC] >2). (**B**) Bubble diagram of biological process (BP) enrichment results. (**C**) Top 9 BP terms corresponding to the top 50 genes by absolute log2 FC. (**D**) Heatmap of genes corresponding to BP terms. (**E**) Bubble diagram of cellular component (CC) enrichment results. (**F**) Top 9 CC terms corresponding to the top 50 genes by absolute log2 FC. (**G**) Heatmap of genes corresponding to CC terms. (**H**) Bubble diagram of molecular function (MF) enrichment results. (**I**) Top 9 MF terms corresponding to the top 50 genes by absolute log2 FC. (**J**) Heatmap of genes corresponding to MF terms.

have mitochondrial dysfunction, imbalance in lactate metabolism, and changes in synaptic plasticity. These characteristics make them both the early targets for hypoxia-induced damage and the key links in amplifying retinal dysfunction and structural degeneration.

Differential Expression Analysis

Differential expression analysis of bipolar cells with the FindMarkers function in the Seurat package revealed 355 upregulated genes and 5 downregulated genes, as shown in **Tables 1 and 2**. These genes are also illustrated in a scatter plot in **Figure 3A**.

GO Enrichment Analysis of DEGs

GO enrichment analysis showed that the top 9 biological process terms were RNA splicing, RNA processing, messenger (m)RNA processing, gene expression, RNA metabolic process, mRNA metabolic process, organelle organization, regulation of RNA metabolic process, and regulation of organelle organization, as shown in **Figure 3B-3D**. The top 9 cellular component terms were nucleus, nucleoplasm, nuclear body, nuclear lumen, nuclear speck, neuron projection, nuclear periphery, spliceosomal complex, and intracellular membrane-bounded organelle, as shown in **Figure 3E-3G**. The top 9 molecular function terms were RNA binding, DNA binding, mRNA binding, kinase binding, mRNA 3' untranslated region binding, histone deacetylase binding, single-stranded DNA binding, lysine-acetylated

Indexed in: [Current Contents/Clinical Medicine] [SCI Expanded] [ISI Alerting System] [ISI Journals Master List] [Index Medicus/MEDLINE] [EMBASE/Excerpta Medica] [Chemical Abstracts/CAS]

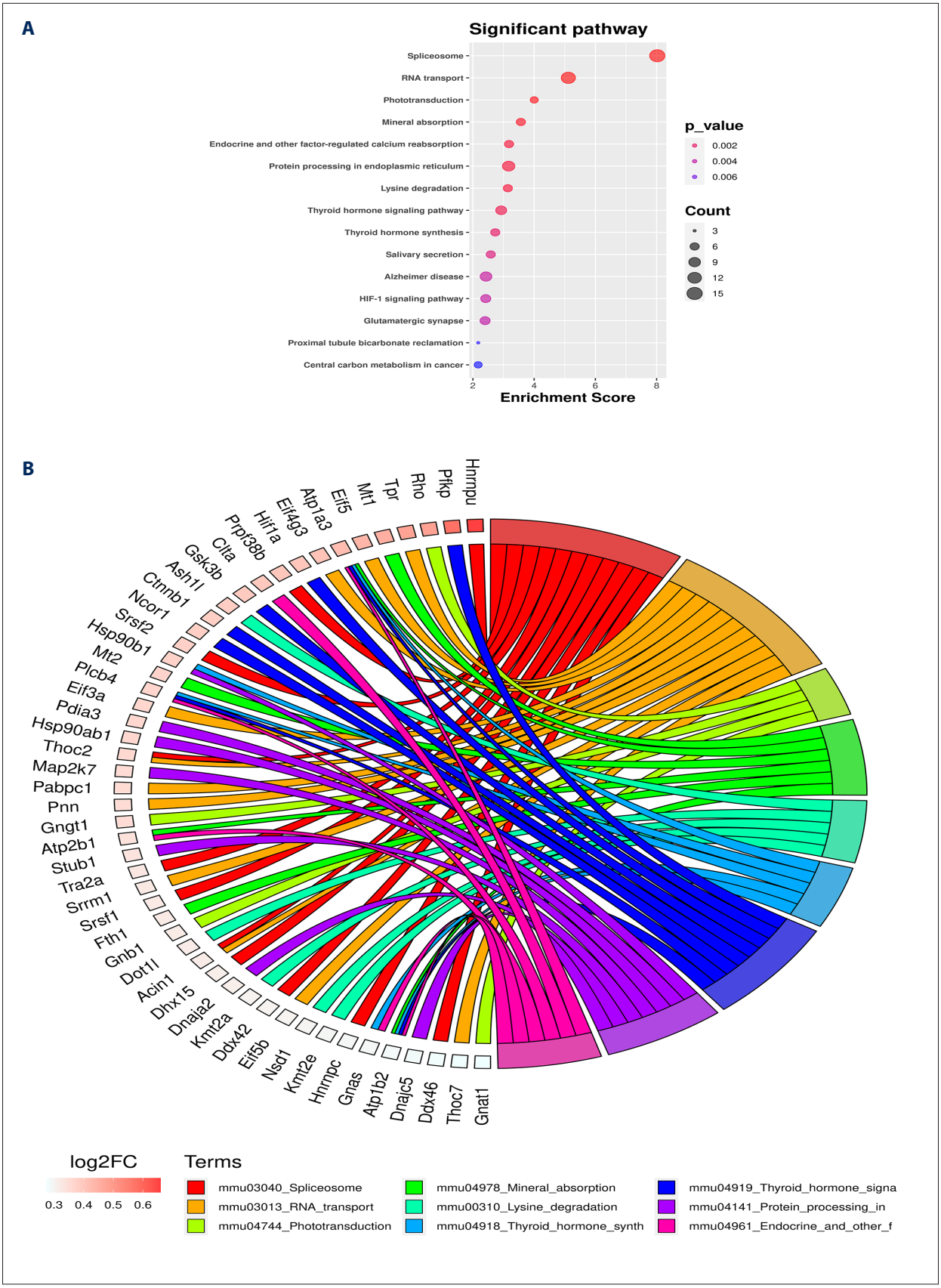

Indexed in: [Current Contents/Clinical Medicine] [SCI Expanded] [ISI Alerting System] [ISI Journals Master List] [Index Medicus/MEDLINE] [EMBASE/Excerpta Medica] [Chemical Abstracts/CAS]

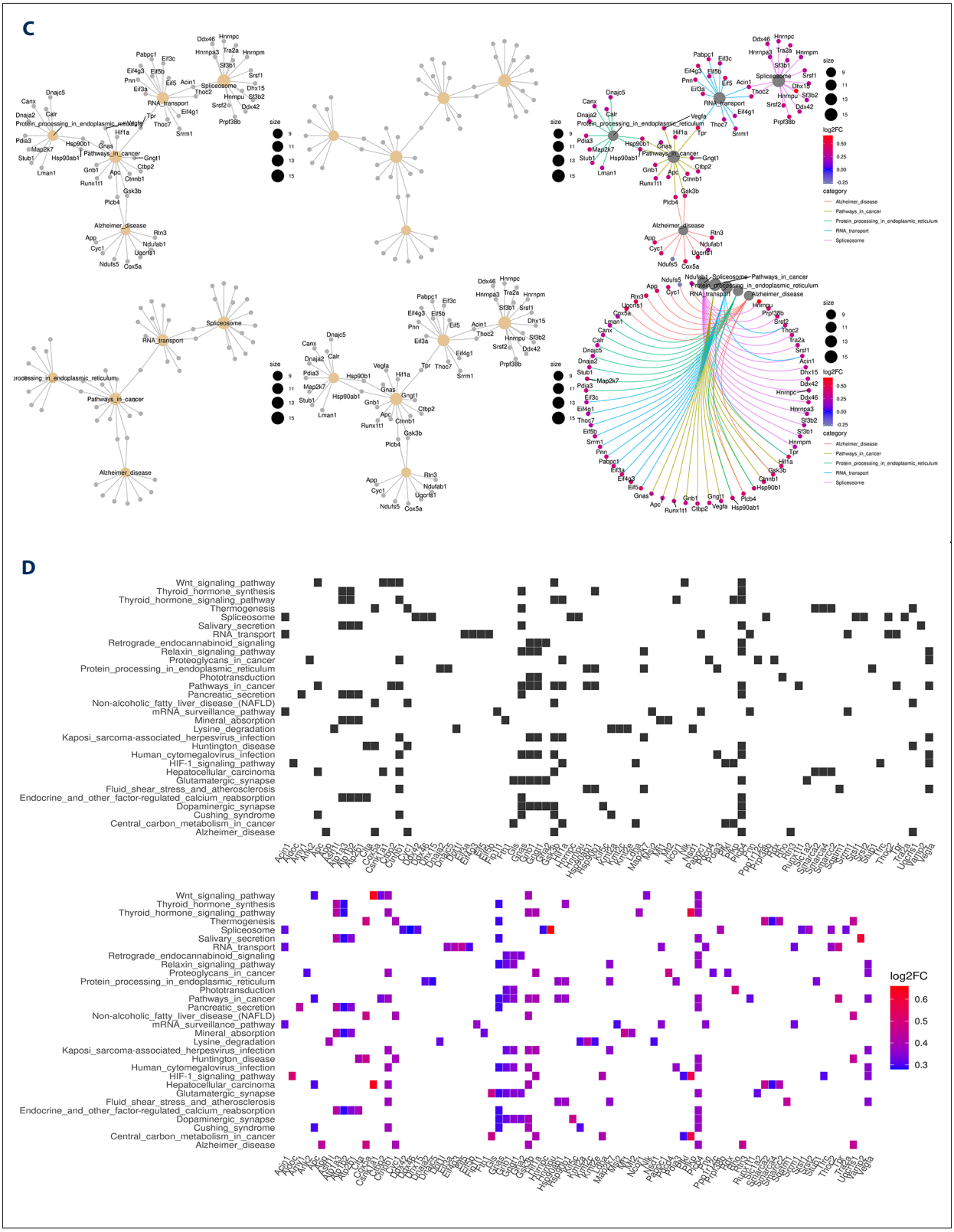

Figure 4. (**A**) Bubble diagram of Kyoto Encyclopedia of Genes and Genomes (KEGG) enrichment results. (**B**) Top 9 KEGG terms corresponding to the top 50 genes by absolute log2 fold change (FC). (**C**) Gene network map corresponding to KEGG terms. (**D**) Heatmap of genes corresponding to KEGG terms.

Indexed in: [Current Contents/Clinical Medicine] [SCI Expanded] [ISI Alerting System] [ISI Journals Master List] [Index Medicus/MEDLINE] [EMBASE/Excerpta Medica] [Chemical Abstracts/CAS]

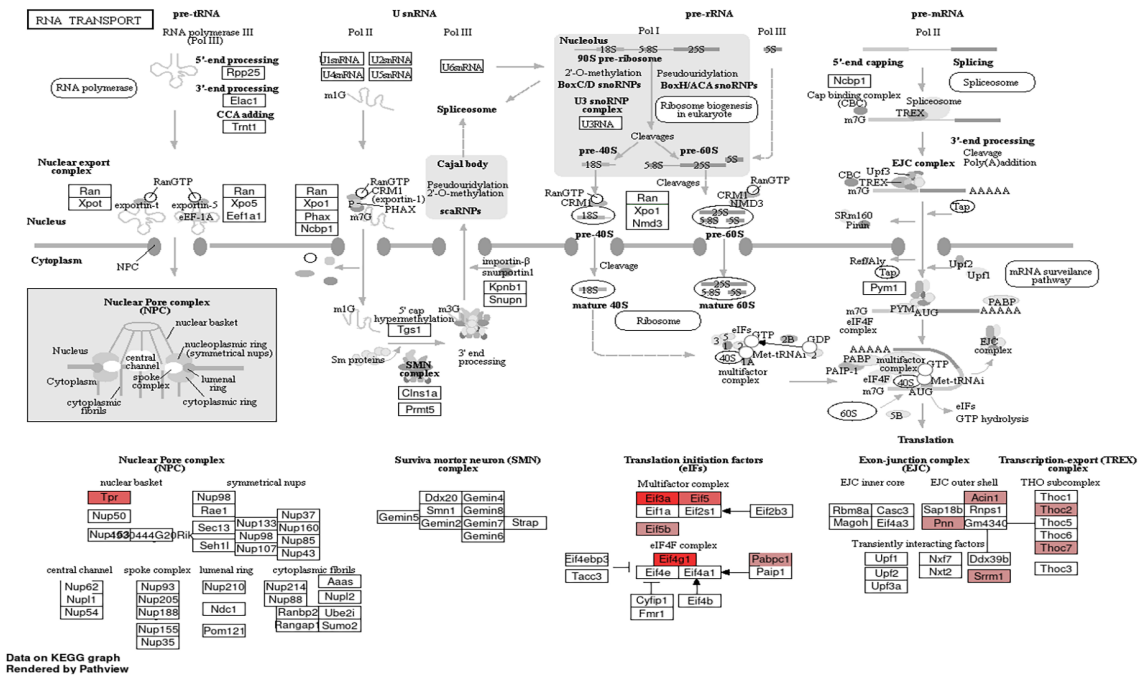

Indexed in: [Current Contents/Clinical Medicine] [SCI Expanded] [ISI Alerting System] [ISI Journals Master List] [Index Medicus/MEDLINE] [EMBASE/Excerpta Medica] [Chemical Abstracts/CAS]

C

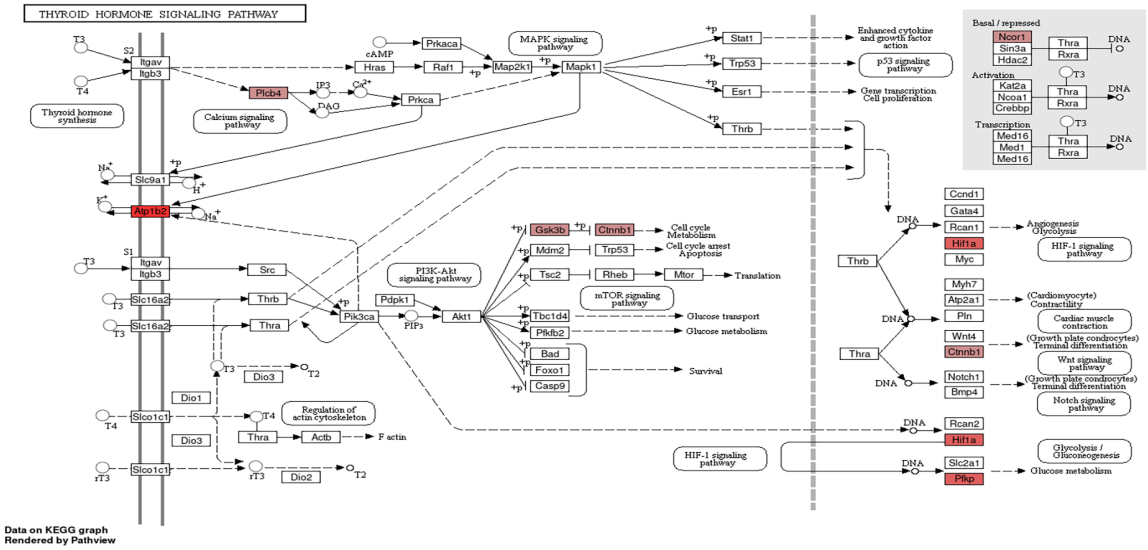

D

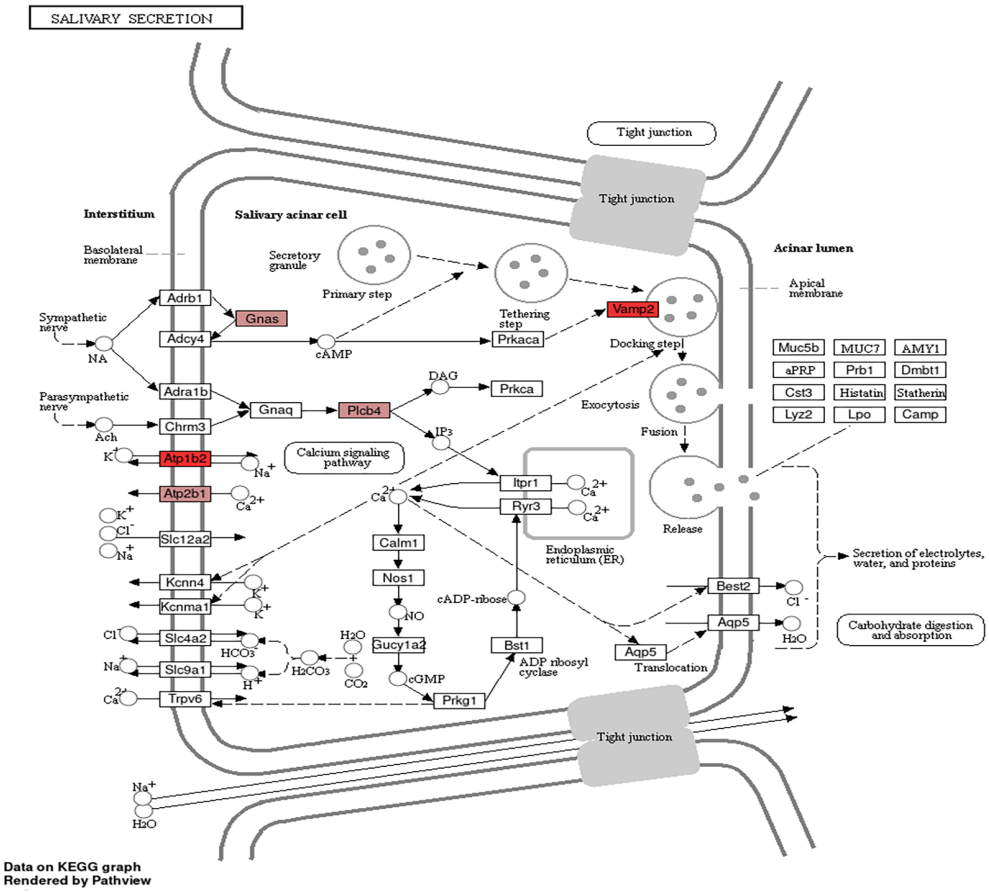

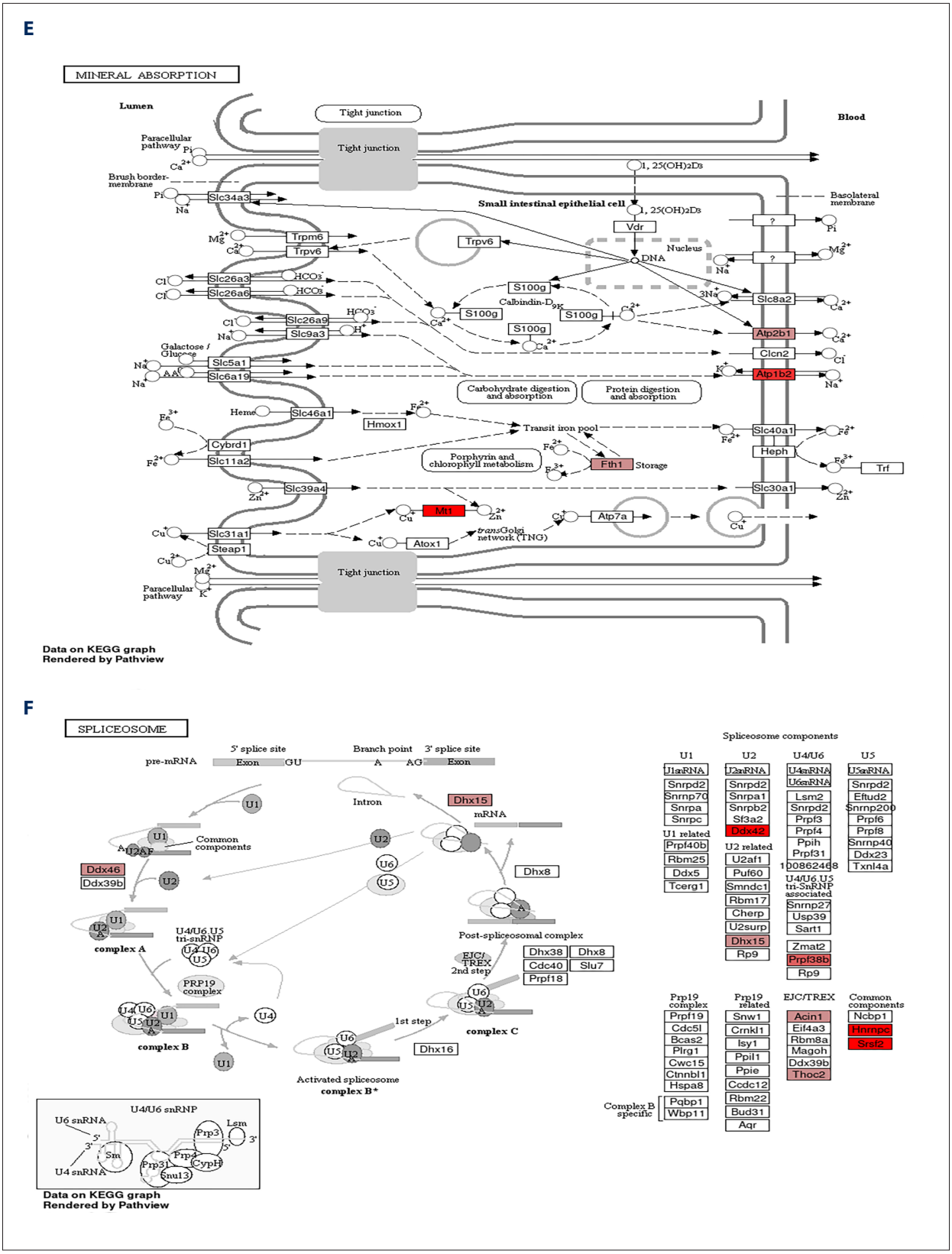

Figure 5. (**A**) RNA transport pathway. (**B**) Phototransduction pathway. (**C**) Thyroid hormone signaling pathway. (**D**) Salivary secretion pathway. (**E**) Mineral absorption pathway. (**F**) Spliceosome pathway.

Indexed in: [Current Contents/Clinical Medicine] [SCI Expanded] [ISI Alerting System] [ISI Journals Master List] [Index Medicus/MEDLINE] [EMBASE/Excerpta Medica] [Chemical Abstracts/CAS]

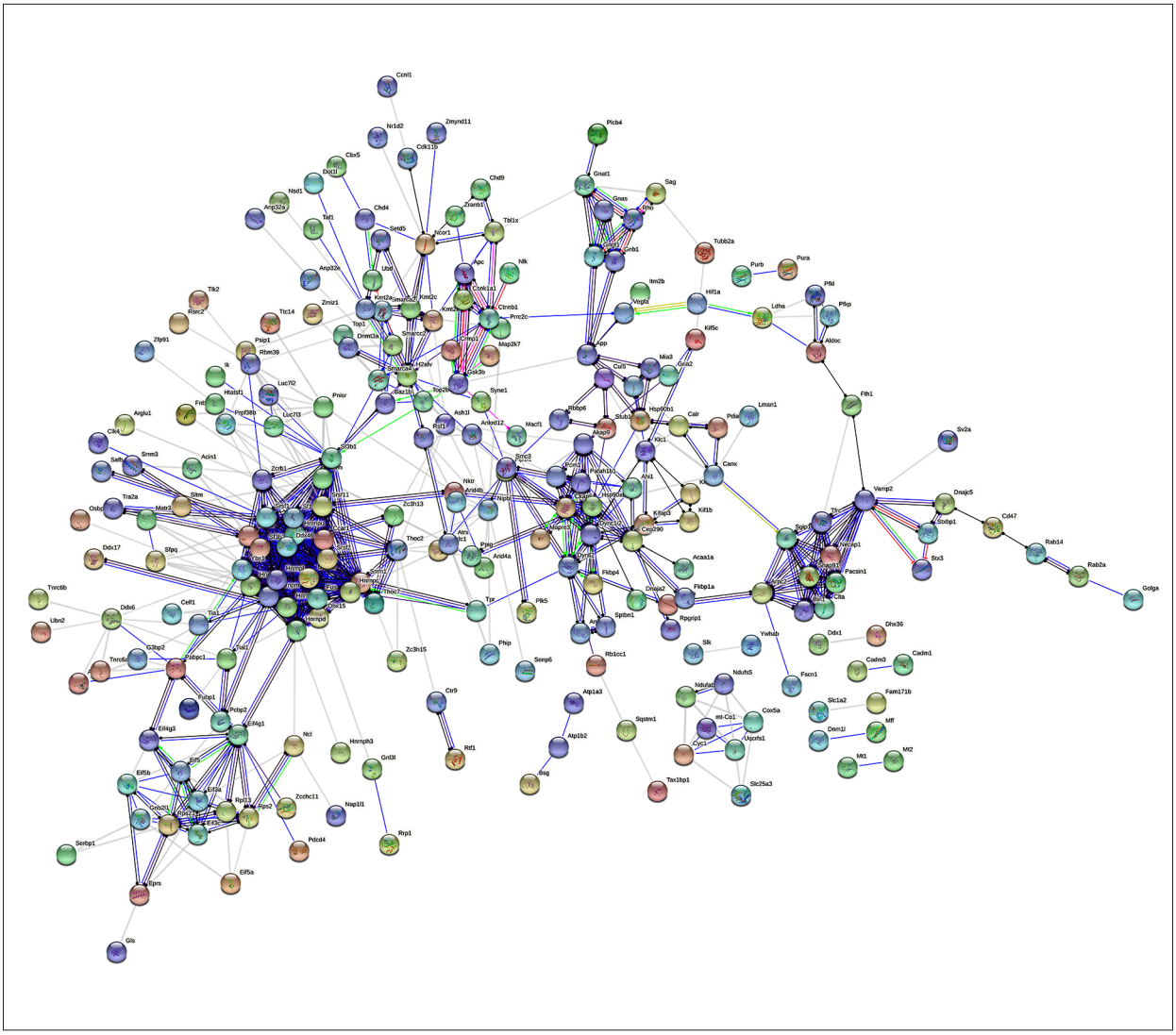

Figure 6. Protein–protein interaction (PPI) network diagram.

histone binding, and nucleoside-triphosphatase activity, as shown in **Figure 3H-3J**.

In GO analysis, the upregulated genes with high expression included Ywhab, heterogeneous nuclear ribonucleoprotein U (Hnrnpu), casein kinase 1 alpha 1 (Csnk1a1), Y-box-binding protein 1 (Ybx1), vesicle-associated membrane protein 2 (Vamp2), purb, and Chchd10, and the downregulated genes included the long noncoding RNA (lncRNA) X-inactive specific transcript (lncRNA Xist) and mitochondrial DNA (mtDNA)-encoded cytochrome c oxidase subunit I (mt-Co1).

KEGG Pathway Enrichment Analysis of DEGs

To characterize the coordinative relations between genes and the roles of the genes in biological functions, the DEGs were subjected to KEGG pathway enrichment analysis, in which biochemical metabolic and signal transduction pathways were found to be enriched. As shown in **Figure 4A**, the top 15 pathways are listed in the bubble plot: spliceosome, RNA transport, phototransduction, mineral absorption, endocrine and other factor-regulated calcium reabsorption, protein processing in endoplasmic reticulum, lysine degradation, thyroid hormone signalling pathway, thyroid hormone synthesis, salivary secretion, Alzheimer disease, HIF-1 signaling pathway, glutamatergic synapse, proximal tubule bicarbonate reclamation, and central carbon metabolism in cancer.

In KEGG analysis, the upregulated genes with high expression included Hnrnpu, phosphofructokinase 1 (Pfkp), Rho, Tpr, Mt1, Vamp2, and Csnk1a1; and the downregulated gene was nicotinamide adenine dinucleotide ubiquinone oxidoreductase subunit 5 (Ndufs5), as shown in **Figure 4B-4D**. The analysis revealed significantly enriched KEGG pathways associated with

Indexed in: [Current Contents/Clinical Medicine] [SCI Expanded] [ISI Alerting System] [ISI Journals Master List] [Index Medicus/MEDLINE] [EMBASE/Excerpta Medica] [Chemical Abstracts/CAS]

Table 3. Gene connectivity table.

Gene	Degree	Gene	Degree	Gene	Degree	Gene	Degree
Srsf1	31	Clta	8	Pfkl	3	Zcchc11	1
Srsf11	30	Cep290	8	Pdia3	3	Ywhab	1
Sf3b1	30	bIN1	8	Pcbp2	3	Ubn2	1
Hnrnpu	26	Ash1l	8	mt-Co1	3	Ttc14	1
Hnrnph1	26	Zcrb1	7	Mia3	3	Tnrc6b	1
Hnrnpc	25	Pcm1	7	Kif5c	3	Tlk2	1
Srsf2	24	Hsp90b1	7	Kif21a	3	Tax1bp1	1
Hnrnpm	24	Gnat1	7	Kif1b	3	Taf1	1
Ybx1	23	Eif5	7	Gnas	3	Sv2a	1
Srrm1	23	bAZ1b	7	Fth1	3	Slk	1
Hnrnpl	23	Uqcrfs1	6	Fkbp4	3	Slc1a2	1
Ddx46	23	Top2b	6	Eif5a	3	Senp6	1
Srrm2	22	Tia1	6	Dnajc5	3	Safb	1
Sf3b2	22	Tbl1x	6	Csnk1a1	3	Rtf1	1
Hnrnpa3	22	Smarca2	6	Chd4	3	Rsrc2	1
Dhx15	22	Sfpq	6	Atxn2l	3	Rrp1	1
Hnrnpd	21	Luc7l3	6	Arid4a	3	Rpgrip1	1
Fus	21	Kmt2e	6	Ank2	3	Purb	1
Ddx42	21	Kmt2c	6	Zc3h15	2	Pura	1
Sf1	20	Eif4g3	6	Ythdc1	2	Plk5	1
Ccar1	20	Cyc1	6	Ubtf	2	Plcb4	1
Dync1i2	14	Cox5a	6	Tubb2a	2	Pdcd4	1
Vamp2	13	Canx	6	Tra2a	2	Osbpl6	1
Nipbl	13	Calr	6	Top1	2	Nsd1	1
H2afv	13	Ahi1	6	Tnrc6a	2	Nr1d2	1
Dynll2	13	Smarcc2	5	Syne1	2	Nlk	1
Pnn	12	Rsf1	5	Stx3	2	Nap1l1	1
Eif4g1	12	Rpl13	5	Srrm3	2	Mt2	1
Thoc2	11	Nktr	5	Sqstm1	2	Mt1	1
Hsp90ab1	11	Matr3	5	Sltm	2	Mff	1
Smc3	10	Kifap3	5	Setd5	2	Map2k7	1
Rps21	10	Gngt1	5	Serbp1	2	Itm2b	1
Ncor1	10	Gnb1	5	Rb1cc1	2	Ik	1
Kmt2a	10	Eprs	5	Rab2a	2	Hnrnph3	1
Eif3a	10	Apc	5	Rab14	2	Golga4	1

Indexed in: [Current Contents/Clinical Medicine] [SCI Expanded] [ISI Alerting System] [ISI Journals Master List] [Index Medicus/MEDLINE] [EMBASE/Excerpta Medica] [Chemical Abstracts/CAS]

Table 3 continued. Gene connectivity table.

Gene	Degree	Gene	Degree	Gene	Degree	Gene	Degree
Atrx	10	Tpr	4	Psip1	2	Gls	1
Arpc2	10	Rho	4	Prrc2c	2	Fubp1	1
App	10	Prpf38b	4	Phip	2	Fscn1	1
Tfrc	9	Ndufs5	4	Myo5a	2	Fkbp1a	1
Sgip1	9	Ndufab1	4	Mapre3	2	Fam171b	1
Rps2	9	Ncl	4	Macf1	2	Dot1l	1
Rbm39	9	Luc7l2	4	Lman1	2	Dnm1l	1
Pnisr	9	Ldha	4	Hif1a	2	Dnaja2	1
Gsk3b	9	Ktn1	4	Gria2	2	Dhx36	1
Gnb2l1	9	Htatsf1	4	Gnl3l	2	Ddx17	1
Eif3c	9	G3bp2	4	Fnbp4	2	Ddx1	1
Ckap5	9	Dnmt3a	4	Fip1l1	2	Crmp1	1
Akap9	9	Arid4b	4	Cul5	2	Clk4	1
Tial1	8	Aldoc	4	Ctr9	2	Ccnl1	1
Thoc7	8	Acin1	4	Chd9	2	Cbx5	1
Snap91	8	Zc3h13	3	Celf1	2	Cadm3	1
Smarca4	8	Vegfa	3	Cdk11b	2	Cadm1	1
Pafah1b1	8	Stxbp1	3	Cd47	2	bsg	1
Pacsin1	8	Stub1	3	Atp1b2	2	Atp1a3	1
Pabpc1	8	Sptbn1	3	Anp32e	2	Arglu1	1
Necap1	8	Slc25a3	3	Ankrd12	2	Anp32a	1
Klc1	8	Sag	3	Zranb1	1	Acaa1a	1
Eif5b	8	Rbbp6	3	Zmynd11	1		
Ddx6	8	Ppig	3	Zmiz1	1		
Ctnnb1	8	Pfkp	3	Zfp91	1		

RNA transport, phototransduction, thyroid hormone signaling, salivary secretion, mineral absorption, and the spliceosome, as presented in **Figures 5A-5E and 6**.

PPI Network Analysis

Based on the above DEGs, PPI network analysis was performed using the STRING online tool. Then, the hub genes were selected based on their connectivity degree, as shown in **Table 3** and **Figure 6**. We identified the genes with a connectivity degree of 25 or greater as hub genes, which included serine/arginine splicing factor 1 (Srsf1), Srsf11, Sf3b1, Hnrnpu, *hnrnph1*, and heterogeneous ribonucleoprotein-C (Hnrnpc).

Discussion

Our research found that genes such as Hnrnpu, Vamp2, Ybx1, Ywhab, Csnk1a1, Pfkp, Rho, Srsf1, Srsf11, Mt1, Tpr, and Hnrnpc are involved in the pathologic angiogenesis in the OIR rat model in the dataset of GSE150703. These genes appeared to be significantly associated with poor outcomes in OIR, suggesting their potential as possible biomarkers for ROP.

ScRNA-seq has found that these genes play some important roles in the pathologic angiogenesis, which agrees with previous studies [18-25]. For example, Hnrnpu is a protein overexpressed in tumor tissues and may influence retinal angiogenesis

Indexed in: [Current Contents/Clinical Medicine] [SCI Expanded] [ISI Alerting System] [ISI Journals Master List] [Index Medicus/MEDLINE] [EMBASE/Excerpta Medica] [Chemical Abstracts/CAS]

by regulating gene expression and cell growth [18,19]. Vamp2 is another protein that may regulate blood vessel permeability during the process of vascular growth [20]. Other proteins like Ybx1 [21], Ywhab [22], and Pfkp [23] are linked to cancer and may also affect neovascularization. Csnk1a1, which helps cells proliferate and form colonies in glioblastoma, could also influence blood vessel development [24]. Rho GTPases are another group that regulate angiogenesis and are involved in processes like permeability, matrix remodeling, and migration [25]. Srsf1 affects processes like epithelial-mesenchymal transition, possibly contributing to pathologic angiogenesis in ROP, including by regulating alternative splicing, influencing cell cycle processes, and potentially driving cell growth or death [26]. Other genes and proteins, such as telomerase, Mt1, Tpr, and Hnrnpc, also contribute to cell survival and growth, and are often linked with poor cancer prognosis [27,28]. In the case of ROP, these proteins could similarly affect cellular balance and contribute to pathologic angiogenesis or neovascularization. These genes, often found to be highly expressed in cancers, point to a commonality between cancer's abnormal blood vessel formation and what happens in ROP. From these studies, and the results of our study, we inferred that the expressions of these genes may closely correlate with the pathologic angiogenesis of ROP. Focusing on the regulation of these genes may help to explore new biomarkers for OIRs.

Chchd10 and Sf3b1 have been reported to be closely associated with cell viability, proliferation, and migration [29,30], and they are also shown to have important PPIs that are critically involved in the formation and progression of OIR in this study. Three mitochondrial-related target genes, lncRNA-Xist, Ndufs5, and mt-Co1, are downregulated in OIR. LncRNA Xist regulates cell growth and development, and its loss promotes cell death in cancer [31,32]. Ndufs5 helps mitochondria work properly, and its reduced activity leads to cell death and potential heart failure [33]. Mt-Co1 is a mitochondrial gene that affects cell death and DNA damage when it is not working correctly [34]. The PPI analysis in the present study showed that these genes may be closely associated with transcription changes in the neovascularization or pathologic angiogenesis in OIR. It is speculated that retinal mitochondrial dysfunction related to these genes may be consistent with the mechanism of retinal ischemia and hypoxia; however, the specific mechanisms require further experimental verification.

The functions of target genes in tumors are consistent with those determined by GO and KEGG enrichment analyses, mainly involving RNA splicing, RNA processing, localization to the nucleus and cytoplasm, RNA binding, RNA transport pathways, spliceosome pathways, AD, HIF-1 signaling pathways, and others. For example, Ybx1 is a binding protein for circRNA-SORE, and silencing circRNA-SORE significantly reduces the protein level of Ybx1 [36]. Srsf1 is a multifunctional protein involved in RNA metabolism-related processes, including transcription, processing, nuclear pore export, and translation of nascent RNA transcripts [37]. Srsf11 is involved in alternative splicing events, and mutations in splicing factors in uveal melanoma generate new antigens uniquely expressed by tumor cells, highlighting the importance of splicing factors as new therapeutic strategies [38]. These studies demonstrate the interactions of these genes in pathological angiogenesis. Our study highlights the role of these genes in OIR pathogenesis, but the findings require further validation.

Limitations

This study identified hub genes related to OIR but has limitations. The study relied on bioinformatics without experimental validation, and the small sample size may limit the generalization of the results. The study also overlooked epigenetic and protein modification interactions and did not fully consider genetic, environmental, and lifestyle factors. Future research should validate findings experimentally and integrate multi-omics data for a more comprehensive understanding of the pathogenesis of ROP.

Conclusions

This study identifies key hub genes in OIR through enrichment and PPI network analyses. These genes, which have been implicated in cancer and immune diseases, are closely associated with the pathological processes of OIR in the present study. These genes may be potential biomarkers for ROP; however, further in vivo experiments or clinical trials are required.

Ethic Approval

This research is a bioinformatics analysis and ethical approval certification is not required.

Research Data and Other Material Availability

The data set GSE150703 and annotation file GPL19057 were downloaded from the Gene Expression Omnibus (GEO) data platform. The relevant data for the research was obtained from the database and analyzed.

Declaration of Figures' Authenticity

All figures submitted have been created by the authors who confirm that the images are original with no duplication and have not been previously published in whole or in part.

Indexed in: [Current Contents/Clinical Medicine] [SCI Expanded] [ISI Alerting System] [ISI Journals Master List] [Index Medicus/MEDLINE] [EMBASE/Excerpta Medica] [Chemical Abstracts/CAS]

References:

1. Filippi L, Gulden S, Cammalleri M, et al. Retinopathy of prematurity in the era of precision neonatology: From risk stratification to targeted therapies. World J Pediatr. 2025;21(5):430-35
2. Dai C, Webster KA, Bhatt A, et al. Concurrent physiological and pathological angiogenesis in retinopathy of prematurity and emerging therapies. Int J Mol Sci. 2021;22(9):4809
3. Fielder AR, Wallace DK, Stahl A, et al. Describing retinopathy of prematurity: Current limitations and new challenges. Ophthalmology. 2019;126(5):652-54
4. Hartnett ME. Pathophysiology of retinopathy of prematurity. Annu Rev Vis Sci. 2023;9:39-70
5. Xu J, Zhang Y, Gan R, et al. Identification and validation of lactate metabolism-related genes in oxygen-induced retinopathy. Sci Rep. 2023;13(1):13319
6. Huang D, Liu Z, Deng Y. Retinopathy of prematurity (ROP): An overview of biomarkers in various samples for prediction, diagnosis, and prognosis. Clin Ophthalmol. 2025;19:1515-30
7. Eraslan G, Simon LM, Mircea M, et al. Single-cell RNA-seq denoising using a deep count autoencoder. Nat Commun. 2019;10(1):390
8. Hsiao CJ, Tung P, Blischak JD, et al. Characterizing and inferring quantitative cell cycle phase in single-cell RNA-seq data analysis. Genome Res. 2020;30(4):611-21
9. Zhao K, Jiang Y, Huang W, et al. Alamandine inhibits pathological retinal neovascularization by targeting the MrgD-mediated HIF-1α/VEGF pathway. J Zhejiang Univ Sci B. 2025;26(10):1015-36
10. Shi S, Xia F, Lu Z, et al. Epac1 deletion attenuates Müller glial pathological activation and mitigates retinal neurodegeneration in ischemia-induced retinopathy. J Adv Res. 2025 [Online ahead of print]
11. Lun ATL, Riesenfeld S, Andrews T, et al. EmptyDrops: Distinguishing cells from empty droplets in droplet-based single-cell RNA sequencing data. Genome Biol. 2019;20:63
12. McCarthy DJ, Campbell KR, Lun AT, Wills QF. Scater: Pre-processing, quality control, normalization and visualization of single-cell RNA-seq data in R. Bioinformatics. 2017;33(8):1179-86
13. Hao Y, Hao S, Andersen-Nissen E, et al. Integrated analysis of multimodal single-cell data. Cell. 2021;184:3573-87.e3529
14. Puthumana J, Thiessen-Philbrook H, Xu L, et al. Biomarkers of inflammation and repair in kidney disease progression. J Clin Invest. 2021;131:e139927
15. Ashburner M, Ball CA, Blake JA, et al. Gene ontology: Tool for the unification of biology. The Gene Ontology Consortium. Nat Genet. 2000;25:25-29
16. Ogata H, Goto S, Sato K, et al. KEGG: Kyoto Encyclopedia of Genes and Genomes. Nucleic Acids Res. 1999;27(1):29-34
17. von Mering C, Huynen M, Jaeggi D, et al. STRING: A database of predicted functional associations between proteins. Nucleic Acids Res. 2003;31(1):258-61
18. Shi ZD, Hao L, Han XX, et al. Targeting HNRNPU to overcome cisplatin resistance in bladder cancer. Mol Cancer. 2022;21:37
19. Liang Y, Fan Y, Liu Y, Fan H. HNRNPU promotes the progression of hepatocellular carcinoma by enhancing CDK2 transcription. Exp Cell Res. 2021;409(1):112898
20. Costa AS, Ferri E, Guerini FR, et al. VAMP2 expression and genotype are possible discriminators in different forms of dementia. Front Aging Neurosci. 2022;14:858162
21. Lasham A, Print CG, Woolley AG, et al. YB-1:Oncoprotein, prognostic marker and therapeutic target? Biochem J. 2013;449(1):11-23
22. Xu C, Du Z, Ren S, et al. MiR-129-5p sensitization of lung cancer cells to etoposide-induced apoptosis by reducing YWHAB. J Cancer. 2020;11(4):858-66
23. Shen J, Jin Z, Lv H, et al. PFKP is highly expressed in lung cancer and regulates glucose metabolism. Cell Oncol (Dordr). 2020;43:617-29
24. Liu G, Li H, Zhang W, et al. Csnk1a1 inhibition modulates the inflammatory secretome and enhances response to radiotherapy in glioma. J Cell Mol Med. 2021;25:7395-406
25. van der Meel R, Symons MH, Kudernatsch R, et al. The VEGF/Rho GTPase signalling pathway: A promising target for anti-angiogenic/anti-invasion therapy. Drug Discov Today. 2011;16:219-28
26. Sokol E, Boguslawska J, Piekielko-Witkowska A. The role of SRSF1 in cancer. Postepy Hig Med Dosw (Online). 2017;71:422-30
27. Lee JH, Jeong SA, Khadka P, et al. Involvement of SRSF11 in cell cycle-specific recruitment of telomerase to telomeres at nuclear speckles. Nucleic Acids Res. 2015;43(17):8435-51
28. Dai H, Wang L, Li L, et al. Metallothionein 1: A new spotlight on inflammatory diseases. Front Immunol. 2021;12:739918
29. Graham JB, Canniff NP, Hebert DN. TPR-containing proteins control protein organization and homeostasis for the endoplasmic reticulum. Crit Rev Biochem Mol Biol. 2019;54:103-18
30. Jian Jiang Y, Jiao B, et al. Genetics of frontotemporal dementia in China. Amyotroph Lateral Scler Frontotemporal Degener. 2021;22(5-6):321-35
31. Zhou Z, Gong Q, Wang Y, et al. The biological function and clinical significance of SF3B1 mutations in cancer. Biomark Res. 2020;8:38
32. Liu J, Yao L, Zhang M, et al. Downregulation of LncRNA-XIST inhibited development of non-small cell lung cancer by activating miR-335/SOD2/ROS signal pathway mediated pyroptotic cell death. Aging (Albany NY). 2019;11(18):7830-46
33. Schilling JD. The mitochondria in diabetic heart failure: From pathogenesis to therapeutic promise. Antioxid Redox Signal. 2015;22:1515-26
34. Martin-Fernandez B, Gredilla R. Mitochondria and oxidative stress in heart aging. Age (Dordr). 2016;38:225-38
35. Sotgia F, Lisanti MP. Mitochondrial biomarkers predict tumor progression and poor overall survival in gastric cancers: Companion diagnostics for personalized medicine. Oncotarget. 2017;8:67117-28
36. Singh RK, Saini SK, Prakasam G, et al. Role of ectopically expressed mtDNA encoded cytochrome C oxidase subunit I (MT-COI) in tumorigenesis. Mitochondrion. 2019;49:56-65
37. Xu J, Ji L, Liang Y, et al. CircRNA-SORE mediates sorafenib resistance in hepatocellular carcinoma by stabilizing YBX1. Signal Transduct Target Ther. 2020;5:298
38. Paz S, Ritchie A, Mauer C, et al. The RNA binding protein SRSF1 is a master switch of gene expression and regulation in the immune system. Cytokine Growth Factor Rev. 2021;57:19-26

Indexed in: [Current Contents/Clinical Medicine] [SCI Expanded] [ISI Alerting System] [ISI Journals Master List] [Index Medicus/MEDLINE] [EMBASE/Excerpta Medica] [Chemical Abstracts/CAS]